Robust Transceiver Design for Covert Integrated Sensing and Communications With Imperfect CSI

Yuchen Zhang, *Graduate Student Member, IEEE*, Wanli Ni, *Member, IEEE*, Jianquan Wang, Wanbin Tang, *Member, IEEE*, Min Jia, *Senior Member, IEEE*, Yonina C. Eldar, *Fellow, IEEE*, and Dusit Niyato, *Fellow, IEEE*

***Abstract*— We propose a robust transceiver design for a covert integrated sensing and communications (ISAC) system with imperfect channel state information (CSI). Considering both bounded and probabilistic CSI error models, we formulate worst-case and outage-constrained robust optimization problems of joint transceiver beamforming and radar waveform design to balance the radar performance of multiple targets while ensuring the communications performance and covertness of the system. The optimization problems are challenging due to the non-convexity arising from the semi-infinite constraints (SICs) and the coupled transceiver variables. In an effort to tackle the former difficulty, S-procedure and Bernstein-type inequality are introduced for converting the SICs into finite convex linear matrix inequalities (LMIs) and second-order cone constraints. A robust alternating optimization framework referred to alternating double-checking is developed for decoupling the transceiver design problem into feasibility-checking transmitter- and receiver-side subproblems, transforming the rank-one constraints into a set of LMIs, and verifying the feasibility of beamforming by invoking the matrix-lifting scheme. Numerical results are provided to demonstrate the effectiveness and robustness of the proposed algorithm in improving the performance of covert ISAC systems.**

***Index Terms*— Integrated sensing and communications, covert communications, robust transceiver design.**

Manuscript received 14 November 2023; revised 9 March 2024; accepted 7 April 2024. Date of publication 12 April 2024; date of current version 18 September 2025. This work was supported in part by the National Natural Science Foundation of China under Grants 62301117 and U19B2014, China Postdoctoral Science Foundation under Grant 2020M683290, and Natural Science Foundation of Xinjiang Uygur Autonomous Region under Grant 2022D01B184. An earlier version of this paper was presented in part at the 2023 IEEE Global Communications Conference (GLOBECOM) [DOI: 10.1109/GLOBECOM54140.2023.10436717]. The associate editor coordinating the review of this article and approving it for publication was S. Buzzi. *(Corresponding author: Jianquan Wang.)*

Yuchen Zhang and Wanbin Tang are with the National Key Laboratory of Wireless Communications, University of Electronic Science and Technology of China, Chengdu 611731, China (e-mail: yc_zhang@std.uestc.edu.cn; wbtang@uestc.edu.cn).

Wanli Ni is with the Department of Electronic Engineering, Tsinghua University, Beijing 100084, China, and also with Beijing National Research Center for Information Science and Technology, Beijing 100084, China (e-mail: niwanli@tsinghua.edu.cn).

Jianquan Wang is with the National Key Laboratory of Wireless Communications, University of Electronic Science and Technology of China, Chengdu 611731, China, and also with Kash Institute of Electronics and Information Industry, Kashgar 844000, China (e-mail: jqwang@uestc.edu.cn).

Min Jia is with the School of Electronics and Information Engineering, Harbin Institute of Technology, Harbin 150008, China (e-mail: jiamin@hit.edu.cn).

Yonina C. Eldar is with the Faculty of Mathematics and Computer Science, Weizmann Institute of Science, Rehovot 7610001, Israel (e-mail: yonina.eldar@weizmann.ac.il).

Dusit Niyato is with the College of Computing and Data Science, Nanyang Technological University, Singapore 639798 (e-mail: dniyato@ntu.edu.sg).

Digital Object Identifier 10.1109/TCOMM.2024.3387869

I. Introduction

DUE to its endogenous dual-functional property, integrated sensing and communications (ISAC), envisioned as a key enabler for next-generation wireless networks, is attracting intensive research efforts from both industry and academia [2]. Compared with traditional radar-communications coexistence, which addresses the spectrum sharing between the two separate systems, ISAC aims to unify the radar and communications functions in one platform. The integration of previously independently designed radar and communications systems can not only improve the efficiency of utilizing increasingly scarce spectrum resource, but also reduce hardware cost through platform reuse. These benefits are continuously stimulating the practical deployment of ISAC techniques such as Wi-Fi sensing and cellular networks-based environmental monitoring.

The challenge of designing an ISAC system is how to make full use of the degrees of freedom (DoFs) at both ends of the transceiver, so as to achieve a better trade-off between radar and communications performance. As a straightforward paradigm, ISAC can be simply realized by orthogonally allocating the temporal, spectral, and spatial resources between existed radar and communications waveforms. However, due to the loose coupling of the two systems, the design DoFs cannot be fully exploited. This gives rise to the study of closely-coupled ISAC wherein a dual-functional waveform achieves the radar and communications functions simultaneously. Thus, in this paper, we focus on the transceiver design of a closely-coupled ISAC system.

A. Related Works

One of the key issues in ISAC is waveform design, which involves designing a waveform that meets the requirements of both radar and communications. This design philosophy can be categorized into three approaches: radar-centric design, communications-centric design, and joint design. The radar-centric design considers radar as the primary function and incorporates communications information into well-designed radar waveforms [3], [4]. On the other hand,

TABLE I
CONTRIBUTIONS IN CONTRAST TO THE STATE-OF-THE-ART

	[7]–[11]	[13]–[17]	[18]	[19]	[20], [21]	[22]	**Proposed**
Multiple radar targets	✓			✓	✓		✓
Imperfect radar channel							✓
Multiple communications users	✓	✓	✓		✓		✓
Imperfect communications channel			✓				✓
Transceiver design		✓	✓	✓	✓		✓
Overt communications	✓	✓	✓	✓	✓		✓
Covert communications						✓	✓
Multiple wardens							✓

communications-centric design exploits existing communications waveforms such as orthogonal frequency division multiplexing waveform to provide radar services [5], [6]. However, the random fluctuations in communications waveforms can adversely affect radar performance reliability. To strike a balance between radar and communications performance, joint design has emerged, leveraging optimization techniques for waveform design. A widely-adopted design criterion is to mimic a promising multiple input multiple output (MIMO) radar beampattern subject to the communications performance requirement by jointly optimizing the MIMO radar and communications waveforms [7], [8], [9], [10], [11]. As a step further, the authors in [12] leveraged Cramér-Rao bound to measure the radar performance, thereby enabling more accurate characterization of the radar-communications performance trade-off in ISAC systems.

The majority of studies have primarily focused on transmitter-side waveform design, with less emphasis on receiver-side filtering/beamforming. Recent research efforts have emerged to explore the untapped potential of radar receivers in enhancing system performance [13], [14], [15], [16], [17], [18], [19], [20], [21]. Different from heuristic metric such as beampattern error adopted in transmitter-side waveform design [7], [8], [9], [10], [11], signal-to-interference-plus-noise ratio (SINR) was usually served as a direct radar performance indicator in the literature of ISAC transceiver design. The authors in [15], [19], and [20] proposed transceiver beamforming designs for multiple-target single-user, single-target multiple-user, and multple-target multiple-user ISAC systems, respectively. Specifically, to enhance the radar SINR, a Capon filter was employed in [15] and [19] for receiver-side beamforming while steering vector of the receive antenna array was matched in [20]. Following works extended the transceiver beamforming designs to various scenarios, e.g., cooperative ISAC network [18] and two-cell interfering ISAC network [16]. The aforementioned designs on ISAC transceiver were based on random waveforms such that the designed statistic such as beamformer only reflects the average performance. However, in some circumstances, deterministic waveform design which accounts for the whole space-time block is necessary given the instantaneous waveform requirements such as constant modulus and low peak-to-average power ratio. With the pursuit of these KPIs, the authors in [13], [14], [17], and [21] studied ISAC transceiver designs under the deterministic waveform regime. In particular, symbol-level precoding, jamming integration, and radar performance balance between multiple targets were further investigated in [14], [17], and [21], respectively.

Due to the potential for the radar targets to be malicious and the broadcasting nature of wireless signals, it is imperative to prioritize security within the realm of ISAC systems. Along with the aforementioned efforts either utilizing the dual-functional benefit or improving the overall performance of ISAC systems, a growing body of research has started to shift its focus towards addressing security concerns. Physical layer security (PLS) aims to prevent the transmitted information from being *decoded* by the eavesdropper. From the perspective of PLS, there have been various studies trying to secure ISAC systems through designing secure dual-functional waveforms [23], [24] or exploiting the artificial noise/interference [25], [26], [27], [28], [29].

B. Motivations and Contributions

As presented in Table I, previous studies have investigated the advantages of receiver-side processing in enhancing the performance of ISAC systems [13], [14], [15], [16], [17], [18], [19], [20], [21]. However, these studies often operate under assumptions of either perfect channel state information (CSI) [19], [20], [21] or scenarios where only communication CSI errors are considered [13], [14], [15], [16], [17], [18]. Consequently, their designs may not be applicable to scenarios where both radar and communication CSIs are imperfect. For example, in [20], the ISAC transceiver was designed to balance radar SINR. However, this approach relies on perfect radar CSI to align the receive beamformer with the steering vector, rendering it inadequate to provide robust performance when radar CSI is inaccurately known. Additionally, when considering imperfect radar CSI, the interdependence between the transmitter and receiver cannot be ignored, further complicating the system design. This highlights the necessity of tailored transceiver designs to ensure robustness in ISAC systems.

Moreover, certain scenarios, such as military and private signal transmission, necessitate not only the protection of transmitted information but also the concealment of the signal's existence. This highlights the necessity for covert communications designed to protect the signal from detection by a warden [22], [30], [31], a service that cannot be provided by PLS. While the PLS of ISAC systems has been

partially addressed in [23], [24], [25], [26], [27], [28], and [29], the exploration of covert communications within ISAC systems is still in its infancy. Recent work in [22] has delved into covert beamforming schemes for ISAC systems, but its focus has been limited to transmitter-side design, overlooking crucial aspects related to receiver-side considerations. Furthermore, the study in [22] only considered a simplified scenario involving a single covert user and radar target. However, the generalization to a more practical scenario, where multiple covert users coexist with multiple overt users and various radar targets, introduces significant challenges [7], [8], [9], [10], [11], [19], [20], [21].

In this paper, we consider transceiver design for a covert ISAC system, and propose robust schemes with imperfect radar and communications CSI. The novelties and contributions are summarized as follows.

- *Versatile Model:* This work marks an early endeavor in integrating covert communications into ISAC systems. Unlike prior studies limited to specific scenarios, our model accommodates multiple overt and covert users as well as radar targets, enhancing versatility. Additionally, unlike most prior ISAC works focusing solely on transmitter-side design, we explore transceiver design, leveraging both transmitter and receiver capabilities simultaneously. To address practical challenges like CSI errors in radar and communication channels, alongside varying availability of historical statistics for CSI errors, we introduce two CSI error models: bounded and probabilistic. By jointly optimizing transmit and receive beamformers and covariance of a dedicated radar waveform, we aim to maximize the minimum radar SINR while ensuring communication SINR and system covertness. Under bounded and probabilistic CSI error models, we conduct worst-case and outage-constrained optimizations, facilitating a comprehensive study of robust ISAC transceiver design.
- *Tailored Method:* The coupled transceiver variables and CSI error-induced semi-infinite constraints (SICs) make the formulated problems non-convex and difficult to solve directly. To overcome these challenges, we utilize the S-procedure and Bernstein-type inequality to convexify the SICs arising from bounded and probabilistic CSI errors, respectively. Furthermore, we develop an optimization framework called alternating double-checking, which applies to both worst-case and outage-constrained designs, addressing the problems by alternately optimizing the transmitter and receiver. Each side is optimized by solving two-step feasibility-checking subproblems. The rank-one property of certain variables is omitted in the first check for convexity, then retrieved in the second check by transforming it into equivalent linear matrix inequalities (LMIs) with an additional bilinear term, which is circumvented through an inner iteration.
- *Useful Insights:* Extensive numerical results confirm the effectiveness of our proposed schemes, offering insights for practical system design. Comparisons with existing approaches, applicable to scenarios with perfect CSI and excluding covert communication, underscore the superiority of our ISAC transceiver design framework. By incorporating covert users and CSI uncertainty, we reveal a tripartite trade-off among radar, overt, and covert communication performances. We demonstrate that the transmit beampattern under radar SINR-oriented transceiver design may not approximate the ideal radar transmit beampattern, thereby highlighting the limitations of the widely-used beampattern-oriented transmitter-side design paradigm.

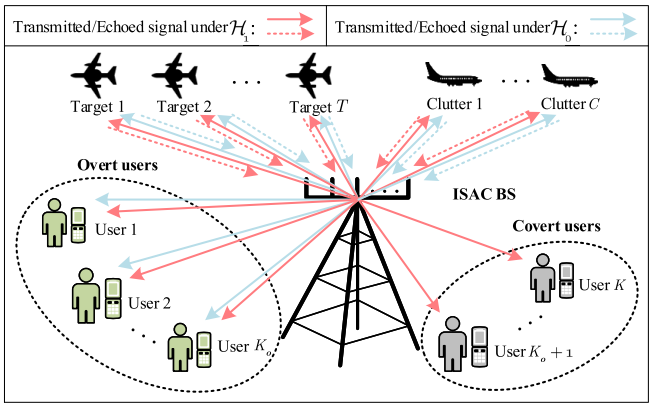

Fig. 1. Illustration of the covert ISAC system with T radar targets, K_o overt communications users, K_c covert communications users, and C signal-dependent clutters.

Notations: The main notations throughout this paper are clarified as follows. Lowercase, bold lowercase, and bold uppercase letters, e.g., a, $\mathbf{a}$, and $\mathbf{A}$, denote a scalar, vector, and matrix, respectively. $|a|$ means the absolute value of a scalar a while $\|\mathbf{a}\|$ means the 2-norm of a vector $\mathbf{a}$. The superscripts T, H, and $*$ denote the transpose, Hermitian transpose, and conjugate transformation of a vector or matrix, respectively. $\mathrm{Diag}(\mathbf{A}_1, \mathbf{A}_2, \ldots, \mathbf{A}_N)$ denotes the matrix which is composed diagonally of matrice $\mathbf{A}_1, \mathbf{A}_2, \ldots, \mathbf{A}_N$. $\mathrm{Tr}(\mathbf{A})$, $\mathrm{Rank}(\mathbf{A})$, and $\mathrm{Vec}(\mathbf{A})$ mean the trace, rank, and vectorization of a matrix $\mathbf{A}$, respectively, while $\mathbf{A} \succeq \mathbf{0}$ means the matrix $\mathbf{A}$ is Hermitian and positive semi-definite. $\mathbf{0}_N$ and $\mathbf{I}_N$ denotes N-dimensional zero and identity matrix, respectively. $\mathbb{E}[\cdot]$ denotes the mathematical expectation. $\mathcal{CN}(\boldsymbol{\mu}, \mathbf{C})$ denotes the circularly symmetric complex Gaussian (CSCG) distribution with mean $\boldsymbol{\mu}$ and covariance matrix $\mathbf{C}$.

II. System Model

As shown in Fig. 1, we consider an ISAC base station (BS) equipped with M_t transmit antennas. The BS is constantly tracking T targets which may be adversarial wardens while communicating with K_o overt single-antenna users. In order to convey messages or commands covertly, the BS intends to communicate with other K_c single-antenna users simultaneously while preventing the communications behaviour from being detected by the wardens.

Let $c_k[n], \forall k \in \mathcal{K}_o = \{1, \ldots, K_o\}$, and $c_k[n], \forall k \in \mathcal{K}_c = \{K_o + 1, \ldots, K_o + K_c\}$, denote the overt and covert data streams at time index $n, \forall n \in \mathcal{N} = \{1, \ldots, N\}$, respectively, where N denote the blocklength. Denote $\mathcal{H}_1$ and $\mathcal{H}_0$ the hypotheses that the BS transmits covert signals or

not, respectively. The transmitted waveforms under hypotheses $\mathcal{H}_1$ and $\mathcal{H}_0$ are structured as the sum of beamformed data streams and a dedicated radar signal. The difference between the transmitted waveforms under hypotheses $\mathcal{H}_1$ and $\mathcal{H}_0$ lies in the inclusion of a signal intended for covert users. Specifically, the transmitted waveform $\mathbf{x}[n] \in \mathbb{C}^{M_t \times 1}$ is given by

$$\begin{cases} \mathcal{H}_1 : \mathbf{x}[n] & = \mathbf{W}_o \mathbf{c}_o[n] + \mathbf{W}_c \mathbf{c}_c[n] + \mathbf{s}[n], \\ \mathcal{H}_0 : \mathbf{x}[n] & = \mathbf{W}_o \mathbf{c}_o[n] + \mathbf{s}[n], \end{cases} \tag{1}$$

where $\mathbf{W}_o = [\mathbf{w}_1, \ldots, \mathbf{w}_{K_o}] \in \mathbb{C}^{M_t \times K_o}$ and $\mathbf{W}_c = [\mathbf{w}_{K_o+1}, \ldots, \mathbf{w}_{K_o+K_c}] \in \mathbb{C}^{M_t \times K_c}$ consist of the transmit beamformers for overt data streams $\mathbf{c}_o[n] = [c_1[n], \ldots, c_{K_o}[n]]^T \in \mathbb{C}^{K_o \times 1}$ and covert data streams $\mathbf{c}_c[n] = [c_{K_o+1}[n], \ldots, c_{K_o+K_c}[n]]^T \in \mathbb{C}^{K_c \times 1}$, respectively. Additionally, $\mathbf{s}[n] \in \mathbb{C}^{M_t \times 1}$ represents the dedicated radar signal.

Let $\mathcal{K} = \mathcal{K}_o \cup \mathcal{K}_c$. It is assumed that $c_k[n], \forall k \in \mathcal{K}$, and $\mathbf{s}[n]$ are independently Gaussian distributed with $c_k[n] \sim \mathcal{CN}(0,1)$ and $\mathbf{s}[n] \sim \mathcal{CN}(\mathbf{0}_{M_t}, \mathbf{R})$, where $\mathbf{R} \in \mathbb{C}^{M_t \times M_t}$ is the positive semidefinite covariance matrix of $\mathbf{s}[n]$. It is noteworthy that introducing $\mathbf{s}[n]$ offers enhanced DoF in waveform design, which can be leveraged to improve the performance of the ISAC system [9], [12], [20].

A. Communications and Radar Performances

Let $\mathbf{h}_{\mathrm{C},k} \in \mathbb{C}^{M_t \times 1}$ denote the communications channel from the BS to the k-th user. Similar to [9] and [25], the received signal at the k-th user under $\mathcal{H}_1$ is given by

$$r_{\mathrm{C},k}[n] = \mathbf{h}_{\mathrm{C},k}^H \mathbf{w}_k c_k[n] + \underbrace{\sum_{i \in \mathcal{K}/k} \mathbf{h}_{\mathrm{C},k}^H \mathbf{w}_i c_i[n]}_{\text{Muti-user interference}} + \underbrace{\mathbf{h}_{\mathrm{C},k}^H \mathbf{s}[n]}_{\text{Radar interference}} + z_{\mathrm{C},k}[n], \tag{2}$$

where $z_{\mathrm{C},k}[n] \sim \mathcal{CN}(0, \sigma_{\mathrm{C},k}^2)$ is the additive white Gaussian noise (AWGN). The communications performance of the k-th user is determined by the SINR given by [25]

$$\gamma_{1,k}^C = \frac{\mathbf{h}_{\mathrm{C},k}^H \mathbf{w}_k \mathbf{w}_k^H \mathbf{h}_{\mathrm{C},k}}{\sum_{i \in \mathcal{K}/k} \mathbf{h}_{\mathrm{C},k}^H \mathbf{w}_i \mathbf{w}_i^H \mathbf{h}_{\mathrm{C},k} + \mathbf{h}_{\mathrm{C},k}^H \mathbf{R} \mathbf{h}_{\mathrm{C},k} + \sigma_{\mathrm{C},k}^2}. \tag{3}$$

Similarly, under $\mathcal{H}_0$, the communications SINR at the k-th user is given by

$$\gamma_{0,k}^C = \frac{\mathbf{h}_{\mathrm{C},k}^H \mathbf{w}_k \mathbf{w}_k^H \mathbf{h}_{\mathrm{C},k}}{\sum_{i \in \mathcal{K}_o/k} \mathbf{h}_{\mathrm{C},k}^H \mathbf{w}_i \mathbf{w}_i^H \mathbf{h}_{\mathrm{C},k} + \mathbf{h}_{\mathrm{C},k}^H \mathbf{R} \mathbf{h}_{\mathrm{C},k} + \sigma_{\mathrm{C},k}^2}. \tag{4}$$

In formulating the received signal at the colocated M_r-antenna receive array, we consider factors that account for T radar targets and C signal-dependent clutters. This corresponds to a practical scenario where the targets we are interested in coexist with interfering entities [15], [19]. Let $\theta_i, \forall i \in \mathcal{T} = \{1, \ldots, T\}$, denote the angles of the targets and $\theta_i, \forall i \in \mathcal{C} = \{T+1, \ldots, T+C\}$, denote the angles of the C clutters. The received signal is expressed as

$$\mathbf{r}_{\mathrm{R}}[n] = \underbrace{\sum_{i \in \mathcal{T}} \alpha_i \mathbf{a}_r^*(\theta_i) \mathbf{a}_t^H(\theta_i) \mathbf{x}[n]}_{\text{Target echo}} + \underbrace{\sum_{i \in \mathcal{C}} \alpha_i \mathbf{a}_r^*(\theta_i) \mathbf{a}_t^H(\theta_i) \mathbf{x}[n]}_{\text{Clutter echo}} + \mathbf{z}_{\mathrm{R}}[n], \tag{5}$$

where α_i represents the complex reflection coefficient that contains both the round-trip path loss and the radar cross-section, and $\mathbf{z}_{\mathrm{R}}[n] \sim \mathcal{CN}(\mathbf{0}, \sigma_{\mathrm{R}}^2 \mathbf{I}_{M_r})$ is the AWGN at the radar receiver. In addition, $\mathbf{a}_t(\theta_i) = [1, \ldots, e^{2\pi(M_t-1)d\cos\theta_i/\lambda}]^T \in \mathbb{C}^{M_t \times 1}$ and $\mathbf{a}_r(\theta_i) = [1, \ldots, e^{2\pi(M_r-1)d\cos\theta_i/\lambda}]^T \in \mathbb{C}^{M_r \times 1}$ are the steering vectors of the transmit and receive antenna arrays, respectively, where d is the antenna interval and λ is the wavelength.

At the BS, the received signal is filtered by a set of receive beamformers to extract the information of the targets such as location and velocity. Both the communications and the dedicated radar waveforms can be exploited as probing signals since they are perfectly known by the BS. Two groups of T receive beamformers should be designed to match the waveforms in (1). Each beamformer in one of the two groups is dedicated to enhance the radar SINR w.r.t. a specific target while treating the signal echoed from other targets and clutters as interference. As in [13], [14], [15], [16], [18], [19], and [20], the ISAC transceiver design relies on radar SINR as the performance metric. Unlike the indirect metrics commonly employed in transmitter-side waveform design, such as beampattern error [7], [8], [9], [10], [11], SINR offers a more direct evaluation of radar target detection and estimation performance [15].

Under $\mathcal{H}_1$, the i-th unit-power receive beamformer w.r.t. the target at θ_i is denoted by $\mathbf{f}_{1,i} \in \mathbb{C}^{M_r \times 1}$. Then, the corresponding radar SINR is given by [19]

$$\gamma_{1,i}^R = \frac{\mathbf{f}_{1,i}^H \mathbf{H}_{\mathrm{R},i} \left(\sum_{k \in \mathcal{K}} \mathbf{w}_k \mathbf{w}_k^H + \mathbf{R}\right) \mathbf{H}_{\mathrm{R},i}^H \mathbf{f}_{1,i}}{\sum_{j \in \mathcal{S}/i} \mathbf{f}_{1,i}^H \mathbf{H}_{\mathrm{R},j} \left(\sum_{k \in \mathcal{K}} \mathbf{w}_k \mathbf{w}_k^H + \mathbf{R}\right) \mathbf{H}_{\mathrm{R},j}^H \mathbf{f}_{1,i} + \sigma_{\mathrm{R}}^2}, \tag{6}$$

where $\mathcal{S} = \mathcal{T} \cup \mathcal{C}$ and $\mathbf{H}_{\mathrm{R},i} = \alpha_i \mathbf{a}_r^*(\theta_i) \mathbf{a}_t^H(\theta_i) \in \mathbb{C}^{M_r \times M_t}$ is the radar round-trip channel. Likewise, the radar SINR under $\mathcal{H}_0$ can be expressed as

$$\gamma_{0,i}^R = \frac{\mathbf{f}_{0,i}^H \mathbf{H}_{\mathrm{R},i} \left(\sum_{k \in \mathcal{K}_o} \mathbf{w}_k \mathbf{w}_k^H + \mathbf{R}\right) \mathbf{H}_{\mathrm{R},i}^H \mathbf{f}_{0,i}}{\sum_{j \in \mathcal{S}/i} \mathbf{f}_{0,i}^H \mathbf{H}_{\mathrm{R},j} \left(\sum_{k \in \mathcal{K}_o} \mathbf{w}_k \mathbf{w}_k^H + \mathbf{R}\right) \mathbf{H}_{\mathrm{R},j}^H \mathbf{f}_{0,i} + \sigma_{\mathrm{R}}^2}, \tag{7}$$

where $\mathbf{f}_{0,i} \in \mathbb{C}^{M_r \times 1}$ is the i-th unit-power receive beamformer w.r.t. the target at θ_i.

B. Detection Performance and Covertness Constraint

We consider the non-colluding scenario where the wardens cannot cooperate with each other. Thus each warden has independent detection performance. The key to ensuring system covertness lies in limiting the detection performance at the

wardens. Specifically, as long as the detection performance at each of the wardens is sufficiently low, they cannot distinguish whether the covert signal exists or not, thereby guaranteeing system covertness.

Let $\mathbf{r}_{\mathrm{W},i} = [r_{\mathrm{W},i}[1], r_{\mathrm{W},i}[2], \ldots, r_{\mathrm{W},i}[N]]^T$ be the received signal at the i-th warden. The hypothesis test at index n is expressed as

$$\begin{cases} \mathcal{H}_1 : r_{\mathrm{W},i}[n] = \beta_i \mathbf{a}_t^H(\theta_i)(\mathbf{W}_o \mathbf{c}_o[n] + \mathbf{W}_c \mathbf{c}_c[n] + \mathbf{s}[n]) \\ \qquad\qquad + z_{\mathrm{W},i}[n], \\ \mathcal{H}_0 : r_{\mathrm{W},i}[n] = \beta_i \mathbf{a}_t^H(\theta_i)(\mathbf{W}_o \mathbf{c}_o[n] + \mathbf{s}[n]) + z_{\mathrm{W},i}[n], \end{cases} \tag{8}$$

where β_i and $z_{\mathrm{W},i}[n] \sim \mathcal{CN}(0, \sigma_{\mathrm{W},i}^2)$ denote the corresponding path loss and AWGN, respectively. Since $r_{\mathrm{W},i}[n], \forall n$, are independently identical distributed, the probability distribution functions (PDFs) of $\mathbf{r}_{\mathrm{W},i}$ under $\mathcal{H}_1$ and $\mathcal{H}_0$ can be easily derived as

$$\mathbb{P}_{1,i} = \mathbb{P}(\mathbf{r}_{\mathrm{W},i}|\mathcal{H}_1) = \frac{\exp\left(-\frac{|\mathbf{r}_{\mathrm{W},i}|^2}{\mathbf{h}_{\mathrm{W},i}^H\left(\sum_{k\in\mathcal{K}} \mathbf{w}_k\mathbf{w}_k^H + \mathbf{R}\right)\mathbf{h}_{\mathrm{W},i} + \sigma_{\mathrm{W},i}^2}\right)}{\pi^N \left(\mathbf{h}_{\mathrm{W},i}^H\left(\sum_{k\in\mathcal{K}} \mathbf{w}_k\mathbf{w}_k^H + \mathbf{R}\right)\mathbf{h}_{\mathrm{W},i} + \sigma_{\mathrm{W},i}^2\right)^N}, \tag{9}$$

and

$$\mathbb{P}_{0,i} = \mathbb{P}(\mathbf{r}_{\mathrm{W},i}|\mathcal{H}_0) = \frac{\exp\left(-\frac{|\mathbf{r}_{\mathrm{W},i}|^2}{\mathbf{h}_{\mathrm{W},i}^H\left(\sum_{k\in\mathcal{K}_o} \mathbf{w}_k\mathbf{w}_k^H + \mathbf{R}\right)\mathbf{h}_{\mathrm{W},i} + \sigma_{\mathrm{W},i}^2}\right)}{\pi^N \left(\mathbf{h}_{\mathrm{W},i}^H\left(\sum_{k\in\mathcal{K}_o} \mathbf{w}_k\mathbf{w}_k^H + \mathbf{R}\right)\mathbf{h}_{\mathrm{W},i} + \sigma_{\mathrm{W},i}^2\right)^N}, \tag{10}$$

respectively, where $\mathbf{h}_{\mathrm{W},i} = \beta_i \mathbf{a}_t(\theta_i) \in \mathbb{C}^{M_t \times 1}$ denotes the detection channel. Note that $\mathbf{h}_{\mathrm{W},i}$ and $\mathbf{H}_{\mathrm{R},i}$ are correlated, as both channels involve $\mathbf{a}_t(\theta_i)$. The implications of this correlation on system design will be further explained latter.

Let $\mathcal{D}_1$ and $\mathcal{D}_0$ represent the decisions in support of $\mathcal{H}_1$ and $\mathcal{H}_0$, respectively. The false alarm probability is defined as $\mathbb{P}_{FA} = \mathbb{P}(\mathcal{D}_1|\mathcal{H}_0)$ while the missed detection probability is defined as $\mathbb{P}_{MD} = \mathbb{P}(\mathcal{D}_0|\mathcal{H}_1)$. Under optimal detection, the warden minimizes the detection error probability $\xi = \mathbb{P}_{FA} + \mathbb{P}_{MD}$ with the minimum denoted by ξ^*. The covertness constraint of the system is expressed as

$$\xi^* = \mathbb{P}_{FA} + \mathbb{P}_{MD} \geq 1 - \epsilon, \tag{11}$$

where $\epsilon \in [0, 1]$ is the covertness constant.

The expression of ξ^* involves complicated gamma functions which leads to a mathematically intractable optimization problem. To circumvent this difficulty, we surrogate ξ^* by its lower bound via leveraging the Kullback-Leibler divergence defined as $\mathcal{D}(\mathbb{P}_{1,i} \,||\, \mathbb{P}_{0,i}) = \int_{\mathbf{r}_{\mathrm{W},i}|\mathcal{H}_1} \mathbb{P}_{1,i} \ln(\frac{\mathbb{P}_{1,i}}{\mathbb{P}_{0,i}}) \mathrm{d}\mathbf{r}_{\mathrm{W},i}$. Based on Pinsker's inequality [32], we have

$$\xi^* \geq 1 - \sqrt{\frac{\mathcal{D}(\mathbb{P}_{1,i} \,||\, \mathbb{P}_{0,i})}{2}}. \tag{12}$$

It is straightforward to verify that the original covertness constraint (11) is fulfilled provided

$$\mathcal{D}(\mathbb{P}_{1,i}||\mathbb{P}_{0,i}) \leq 2\epsilon^2. \tag{13}$$

Furthermore, by substituting (9) and (10) into the expression of $\mathcal{D}(\mathbb{P}_{1,i}||\mathbb{P}_{0,i})$, we have $\mathcal{D}(\mathbb{P}_{1,i}||\mathbb{P}_{0,i}) = Nf\left(\frac{\mathbf{h}_{\mathrm{W},i}^H\left(\sum_{k\in\mathcal{K}_c} \mathbf{w}_k\mathbf{w}_k^H\right)\mathbf{h}_{\mathrm{W},i}}{\mathbf{h}_{\mathrm{W},i}^H\left(\sum_{k\in\mathcal{K}_o} \mathbf{w}_k\mathbf{w}_k^H + \mathbf{R}\right)\mathbf{h}_{\mathrm{W},i} + \sigma_{\mathrm{W},i}^2}\right)$, where the function $f(x) = x - \ln(1+x)$ is monotonically increasing for $x \geq 0$. Then, the covertness constraint in (13) can be simplified as

$$\mathbf{h}_{\mathrm{W},i}^H \mathbf{\Xi} \mathbf{h}_{\mathrm{W},i} \leq \eta\sigma_{\mathrm{W},i}^2, \tag{14}$$

where $\mathbf{\Xi} = \sum_{k\in\mathcal{K}_c} \mathbf{w}_k\mathbf{w}_k^H - \eta\left(\sum_{k\in\mathcal{K}_o} \mathbf{w}_k\mathbf{w}_k^H + \mathbf{R}\right) \in \mathbb{C}^{M_t \times M_t}$ and $\eta \geq 0$ is the solution of $f(x) = \frac{2\epsilon^2}{N}$. Specifically, when $\epsilon = 0$, $\eta = 0$.

C. Channel Error Model

The considered covert ISAC system involves three types of channels including the communications channels $\mathbf{h}_{\mathrm{C},k}, \forall k \in \mathcal{K}$, detection channels $\mathbf{h}_{\mathrm{W},i}, \forall i \in \mathcal{T}$, and radar round-trip channel $\mathbf{H}_{\mathrm{R},j}, \forall j \in \mathcal{S}$. In practice, due to inevitable errors arising from estimation or quantization, the CSI of the communications channel cannot be perfectly known at the BS [33], [34]. Additionally, the directions of the targets are unlikely to be perfectly known, introducing certain degree of ambiguities in the angles [25], [28]. Moreover, the RCSs of the targets are also unlikely to be perfectly estimated. Both factors lead to imperfect radar CSI. Instead of assuming perfect CSI or solely considering imperfect communications CSI as studies summarized in Table I, we aim to investigate the scenario where both the radar and communications channels are imperfectly known at the BS. The CSIs of the three kinds of channels are expressed as the sum of the estimated value and estimation error, i.e., $\mathbf{h}_{\mathrm{C},k} = \widetilde{\mathbf{h}}_{\mathrm{C},k} + \Delta\mathbf{h}_{\mathrm{C},k}$, $\mathbf{h}_{\mathrm{W},i} = \widetilde{\mathbf{h}}_{\mathrm{W},i} + \Delta\mathbf{h}_{\mathrm{W},i}$, and $\mathbf{H}_{\mathrm{R},j} = \widetilde{\mathbf{H}}_{\mathrm{R},j} + \Delta\mathbf{H}_{\mathrm{R},j}$, respectively. The accuracy of the CSI has a significant impact on the performance of the system. In the following, we introduce two types of the CSI error model.

- *Bounded CSI error*: The norms of the CSI errors are bounded by known constants $e_{\mathrm{C},k}^2$, $e_{\mathrm{W},i}^2$, and $e_{\mathrm{R},j}^2$, respectively, i.e.,

$$\Delta\mathbf{h}_{\mathrm{C},k} \in \mathrm{C}_k, \quad \forall k \in \mathcal{K}, \tag{15a}$$
$$\Delta\mathbf{h}_{\mathrm{W},i} \in \mathrm{W}_i, \quad \forall i \in \mathcal{T}, \tag{15b}$$
$$\mathrm{Vec}(\Delta\mathbf{H}_{\mathrm{R},j}) \in \mathrm{R}_j, \quad \forall j \in \mathcal{S}, \tag{15c}$$

  where $\mathrm{C}_k = \{\Delta\mathbf{h}_{\mathrm{C},k} | \|\Delta\mathbf{h}_{\mathrm{C},k}\|^2 \leq e_{\mathrm{C},k}^2\}$, $\mathrm{W}_i = \{\Delta\mathbf{h}_{\mathrm{W},i} | \|\Delta\mathbf{h}_{\mathrm{W},i}\|^2 \leq e_{\mathrm{W},i}^2\}$, and $\mathrm{R}_j = \{\mathrm{Vec}(\Delta\mathbf{H}_{\mathrm{R},j}) | \|\mathrm{Vec}(\Delta\mathbf{H}_{\mathrm{R},j})\|^2 \leq e_{\mathrm{R},j}^2\}$.
- *Probabilistic CSI error*: The CSI error vectors are characterized by a CSCG distribution with a known covariance matrix, i.e.,

$$\Delta\mathbf{h}_{\mathrm{C},k} \sim \mathcal{CN}(\mathbf{0}, \mathbf{E}_{\mathrm{C},k}), \quad \forall k \in \mathcal{K}, \tag{16a}$$
$$\Delta\mathbf{h}_{\mathrm{W},i} \sim \mathcal{CN}(\mathbf{0}, \mathbf{E}_{\mathrm{W},i}), \quad \forall i \in \mathcal{T}, \tag{16b}$$
$$\mathrm{Vec}(\Delta\mathbf{H}_{\mathrm{R},j}) \sim \mathcal{CN}(\mathbf{0}, \mathbf{E}_{\mathrm{R},j}), \quad \forall j \in \mathcal{S}, \tag{16c}$$

where $\mathbf{E}_{\mathrm{C},k} \in \mathbb{C}^{M_t \times M_t}$, $\mathbf{E}_{\mathrm{W},i} \in \mathbb{C}^{M_t \times M_t}$, and $\mathbf{E}_{\mathrm{R},j} \in \mathbb{C}^{M_t M_r \times M_t M_r}$ are positive semidefinite error covariance matrices.

III. Worst-Case Robust Design Under Bounded Error Model

In this section, we investigate the worst-case robust transceiver design under bounded error model. To be specific, we aim to maximize the minimum radar SINR among all targets subject to fulfilling the communications rate requirement and covertness constraint over all possible channel realizations.[1] The formulated problem is non-convex, which is recast into a SDP problem with rank-one constraints. Then, we present a matrix-lifting approach to reformulate the rank-one constraints, and propose an AO-based algorithm to solve this problem.

A. Problem Formulation

We aim to maximize the minimum radar SINR among targets subject to fulfilling the communications SINR requirement and covertness constraint[2] over possible channel realizations. We can verify that $\gamma_{1,k}^C \le \gamma_{0,k}^C$ from (3) and (4). The communications SINR and transmit power are limited by those under $\mathcal{H}_1$. Therefore, the optimization problem w.r.t. the transmit and receive beamformers and the radar covariance matrix is formulated as

$$\max_{\mathbf{w}_k,\mathbf{R},\mathbf{f}_{1,i},\mathbf{f}_{0,i}} \min_{i\in\mathcal{T}} \min_{\mathrm{Vec}(\Delta\mathbf{H}_{\mathrm{R},j})\in\mathrm{R}_j} \left\{\gamma_{1,i}^R, \gamma_{0,i}^R\right\} \tag{17a}$$

$$\text{s.t.} \quad \gamma_{1,k}^C \ge \Gamma_k, \forall \Delta\mathbf{h}_{\mathrm{C},k} \in \mathrm{C}_k, k \in \mathcal{K}, \tag{17b}$$

$$\mathbf{h}_{\mathrm{W},i}^H \mathbf{\Xi} \mathbf{h}_{\mathrm{W},i} \le \eta\sigma_{\mathrm{W},i}^2, \quad \forall \Delta\mathbf{h}_{\mathrm{W},i} \in \mathrm{W}_i, i \in \mathcal{T}, \tag{17c}$$

$$\mathrm{Tr}\left(\sum_{k\in\mathcal{K}} \mathbf{w}_k\mathbf{w}_k^H + \mathbf{R}\right) \le P, \tag{17d}$$

$$\mathrm{Tr}\left(\mathbf{f}_{1,i}\mathbf{f}_{1,i}^H\right) = 1, \mathrm{Tr}\left(\mathbf{f}_{0,i}\mathbf{f}_{0,i}^H\right) = 1, \forall i \in \mathcal{T}, \tag{17e}$$

$$\mathbf{R} \succeq \mathbf{0}, \tag{17f}$$

where $\Gamma_1, \ldots, \Gamma_{K_o}$ and $\Gamma_{K_o+1}, \ldots, \Gamma_{K_o+K_c}$ denote the targeted SINRs for the overt and covert communications, respectively, and P is the power budget.

In (17a), the minimum radar SINR among targets is indicated by $\min_{i\in\mathcal{T}}$. Furthermore, to ensure robustness, the minimum radar SINR should be selected considering various channel realizations. Additionally, since different receive beamformers $\mathbf{f}_{1,i}$ and $\mathbf{f}_{0,i}$ are designed under hypotheses $\mathcal{H}_1$ and $\mathcal{H}_0$ to match different transmitted waveforms, the minimum radar SINR should be further determined from $\gamma_{1,i}^R$ and $\gamma_{0,i}^R$. These considerations are integrated into $\min_{\mathrm{Vec}(\Delta\mathbf{H}_{\mathrm{R},j})\in\mathrm{R}_j} \left\{\gamma_{1,i}^R, \gamma_{0,i}^R\right\}$.

To be noted, while the covertness constraint (17c) can be met with sufficiently low transmit power, the communication SINR requirement (17b) necessitates sufficiently high power at the users. When channels between covert users and wardens are well-aligned, these conflicting requirements may lead to no feasible solution. Actually, if the communication SINR requirement Γ_k is too large, (17b) alone can render the problem infeasible. This point will be confirmed in the numerical results.

B. Problem Reformulation

To tackle the SICs (17b) and (17c), we introduce the following lemma.

Lemma 1: (S-Procedure [34]): Define the quadratic functions w.r.t. $\mathbf{x} \in \mathbb{C}^{M\times 1}$ *as*

$$f_m(\mathbf{x}) = \mathbf{x}^H\mathbf{A}_m\mathbf{x} + 2Re\left\{\mathbf{b}_m^H\mathbf{x}\right\} + c_m, m = 1, 2, \tag{18}$$

where $\mathbf{A}_m \in \mathbb{C}^{M\times M}$, $\mathbf{b}_m \in \mathbb{C}^{M\times 1}$, *and* $c_m \in \mathbb{R}$. *The condition* $f_1 \le 0 \Rightarrow f_2 \le 0$ *holds if and only if there exists a variable* $\omega \ge 0$ *such that*

$$\omega\begin{bmatrix}\mathbf{A}_1 & \mathbf{b}_1\\ \mathbf{b}_1^H & c_1\end{bmatrix} - \begin{bmatrix}\mathbf{A}_2 & \mathbf{b}_2\\ \mathbf{b}_2^H & c_2\end{bmatrix} \succeq \mathbf{0}_{M+1}. \tag{19}$$

Note that $\Delta\mathbf{h}_{\mathrm{C},k} \in \mathrm{C}_k$ leads to $\Delta\mathbf{h}_{\mathrm{C},k}^H\Delta\mathbf{h}_{\mathrm{C},k} \le e_{\mathrm{C},k}^2$. By substituting $\mathbf{h}_{\mathrm{C},k} = \widetilde{\mathbf{h}}_{\mathrm{C},k} + \Delta\mathbf{h}_{\mathrm{C},k}$ into (17b), $\gamma_{1,k}^C \ge \Gamma_k$ can be transformed into

$$\Delta\mathbf{h}_{\mathrm{C},k}^H\mathbf{\Psi}_k\Delta\mathbf{h}_{\mathrm{C},k} + 2\mathbf{\Psi}_k\widetilde{\mathbf{h}}_{\mathrm{C},k} - \Gamma_k\sigma_{\mathrm{C},k}^2 + \widetilde{\mathbf{h}}_{\mathrm{C},k}^H\mathbf{\Psi}_k\widetilde{\mathbf{h}}_{\mathrm{C},k} \ge 0, \tag{20}$$

where $\mathbf{\Psi}_k = \mathbf{W}_k - \sum_{q=1,q\ne k}^{K_o+K_c}\Gamma_k\mathbf{W}_q - \Gamma_k\mathbf{R} \in \mathbb{C}^{M_t\times M_t}$ with $\mathbf{W}_k = \mathbf{w}_k\mathbf{w}_k^H \in \mathbb{C}^{M_t\times M_t}$. According to Lemma 1, (17b) is equivalent to

$$\begin{bmatrix}\mu_k\mathbf{I} + \mathbf{\Psi}_k & \mathbf{\Psi}_k\widetilde{\mathbf{h}}_{\mathrm{C},k}\\ \widetilde{\mathbf{h}}_{\mathrm{C},k}^H\mathbf{\Psi}_k & \widetilde{\mathbf{h}}_{\mathrm{C},k}^H\mathbf{\Psi}_k\widetilde{\mathbf{h}}_{\mathrm{C},k} - \Gamma_k\sigma_{\mathrm{C},k}^2 - \mu_k e_{\mathrm{C},k}^2\end{bmatrix} \succeq \mathbf{0}, \quad \mu_k \ge 0, \forall k \in \mathcal{K}, \tag{21}$$

where μ_k is the introduced auxiliary variable.

Similarly, the constraint (17c) can be transformed into

$$\begin{bmatrix}\phi_i\mathbf{I} - \mathbf{\Xi} & -\mathbf{\Xi}\widetilde{\mathbf{h}}_{\mathrm{W},i}\\ -\widetilde{\mathbf{h}}_{\mathrm{W},i}^H\mathbf{\Xi} & \eta\sigma_{\mathrm{W},i}^2 - \widetilde{\mathbf{h}}_{\mathrm{W},i}^H\mathbf{\Xi}\widetilde{\mathbf{h}}_{\mathrm{W},i} - \phi_i e_{\mathrm{W},i}^2\end{bmatrix} \succeq \mathbf{0}, \quad \phi_i \ge 0, \forall i \in \mathcal{T}, \tag{22}$$

where ϕ_i is the introduced auxiliary variable.

Next, in order to handle the complicated max-min objective function, we introduce an auxiliary variable $t = \min_{i\in\mathcal{T}} \min_{\mathrm{Vec}(\Delta\mathbf{H}_{\mathrm{R},j})\in\mathrm{R}_j} \{\gamma_{1,i}^R, \gamma_{0,i}^R\}$ as the lower bound of radar SINR. Define $\mathbf{F}_{1,i} = \mathbf{f}_{1,i}\mathbf{f}_{1,i}^H \in \mathbb{C}^{M_r\times M_r}$ and $\mathbf{F}_{0,i} = \mathbf{f}_{0,i}\mathbf{f}_{0,i}^H \in \mathbb{C}^{M_r\times M_r}$. The objective function (17a) can be reformulated as

$$\max_{\mathbf{W}_k,\mathbf{R},\mathbf{F}_{1,i},\mathbf{F}_{0,i},t} \quad t \tag{23a}$$

$$\text{s.t.} \quad \gamma_{1,i}^R \ge t, \gamma_{0,i}^R \ge t, \quad \mathrm{Vec}(\Delta\mathbf{H}_{\mathrm{R},j}) \in \mathrm{R}_j, \forall i \in \mathcal{T}, j \in \mathcal{S}. \tag{23b}$$

[1] To maximize radar SINR, the transceiver should be designed to align transmit and receive steering vectors simultaneously. This alignment may lead to a significant power boost towards the targets due to the correlation between $\mathbf{H}_{\mathrm{R},i}$ and $\mathbf{h}_{\mathrm{W},i}$, which intuitively enhances the detection performance of the targets and undermines covertness. Nevertheless, achieving covertness does not rely on minimizing the absolute power, but rather on managing the difference. Detection by the warden depends on a hypothesis test, where the presence of the covert signal distinguishes between hypotheses. Aligning beamformers for covert users with null space relative to warden channels reduces power differentials, ensuring covertness.

[2] In practice, guarantying communication performance and system covertness typically necessitates controlling quality of service (QoS) via SINR thresholds and covertness constants. Meanwhile, the critical radar task aims to maximize performance, underpinning the rationale behind the proposed radar-centric robust ISAC transceiver design.

By applying linear manipulations, the radar SINRs under $\mathcal{H}_1$ and $\mathcal{H}_0$ can be transformed into as in (24) and (25), shown at the bottom of the page, respectively. Moreover, we define $\widetilde{\mathbf{g}}_{\mathrm{R}} = [\mathrm{Vec}(\widetilde{\mathbf{H}}_{\mathrm{R},1}), \ldots, \mathrm{Vec}(\widetilde{\mathbf{H}}_{\mathrm{R},T+C})]^T \in \mathbb{C}^{(T+C)M_tM_r\times 1}$, $\Delta\mathbf{g}_{\mathrm{R}} = [\mathrm{Vec}(\Delta\mathbf{H}_{\mathrm{R},1}), \ldots, \mathrm{Vec}(\Delta\mathbf{H}_{\mathrm{R},T+C})]^T \in \mathbb{C}^{(T+C)M_tM_r\times 1}$, and $\mathrm{R} = \{\Delta\mathbf{g}_{\mathrm{R}} | \|\Delta\mathbf{g}_{\mathrm{R}}\|^2 \le e_{\mathrm{R}}^2 = \sum_{j\in\mathcal{S}} e_{\mathrm{R},j}^2\}$. Then, (23b) is recast as the quadratic forms

$$\begin{aligned}
&\Delta\mathbf{g}_{\mathrm{R}}^H\mathbf{X}_{1,i}\Delta\mathbf{g}_{\mathrm{R}} + 2\mathrm{Re}\left\{\left(\mathbf{X}_{1,i}\widetilde{\mathbf{g}}_{\mathrm{R}}\right)^H\Delta\mathbf{g}_{\mathrm{R}}\right\} + \widetilde{\mathbf{g}}_{\mathrm{R}}^H\mathbf{X}_{1,i}\widetilde{\mathbf{g}}_{\mathrm{R}} \\
&\quad + \sigma_{\mathrm{R}}^2 \le 0, \\
&\Delta\mathbf{g}_{\mathrm{R}}^H\mathbf{X}_{0,i}\Delta\mathbf{g}_{\mathrm{R}} + 2\mathrm{Re}\left\{\left(\mathbf{X}_{0,i}\widetilde{\mathbf{g}}_{\mathrm{R}}\right)^H\Delta\mathbf{g}_{\mathrm{R}}\right\} + \widetilde{\mathbf{g}}_{\mathrm{R}}^H\mathbf{X}_{0,i}\widetilde{\mathbf{g}}_{\mathrm{R}} \\
&\quad + \sigma_{\mathrm{R}}^2 \le 0, \Delta\mathbf{g}_{\mathrm{R}} \in \mathrm{R}, \forall i \in \mathcal{T},
\end{aligned} \tag{26}$$

where

$$\begin{aligned}
\mathbf{X}_{1,i} = \mathrm{Diag}\Bigg(&\left(\sum_{k\in\mathcal{K}}\mathbf{W}_k + \mathbf{R}\right)^* \otimes \mathbf{F}_{1,i}, \ldots, \mathbf{D}_{1,i}, \\
&\ldots, \left(\sum_{k\in\mathcal{K}}\mathbf{W}_k + \mathbf{R}\right)^* \otimes \mathbf{F}_{1,i}\Bigg)
\end{aligned} \tag{27}$$

and

$$\begin{aligned}
\mathbf{X}_{0,i} = \mathrm{Diag}\Bigg(&\left(\sum_{k\in\mathcal{K}_o}\mathbf{W}_k + \mathbf{R}\right)^* \otimes \mathbf{F}_{0,i}, \ldots, \mathbf{D}_{0,i}, \\
&\ldots, \left(\sum_{k\in\mathcal{K}_o}\mathbf{W}_k + \mathbf{R}\right)^* \otimes \mathbf{F}_{0,i}\Bigg).
\end{aligned} \tag{28}$$

Additionally, the i-th matrices of $\mathbf{X}_{1,i}$ and $\mathbf{X}_{0,i}$ are given by $\mathbf{D}_{1,i} = -(\sum_{k\in\mathcal{K}}\mathbf{W}_k + \mathbf{R})^* \otimes \mathbf{F}_{1,i}/t \in \mathbb{C}^{M_tM_r\times M_tM_r}$ and $\mathbf{D}_{0,i} = -(\sum_{k\in\mathcal{K}_o}\mathbf{W}_k + \mathbf{R})^* \otimes \mathbf{F}_{0,i}/t \in \mathbb{C}^{M_tM_r\times M_tM_r}$, respectively. Again, based on the above formulations, we can leverage Lemma 1 to transform (26) into LMIs as

$$\begin{aligned}
&\begin{bmatrix} \varpi_{1,i}\mathbf{I} - \mathbf{X}_{1,i} & -\mathbf{X}_{1,i}\widetilde{\mathbf{g}}_{\mathrm{R}} \\ -\widetilde{\mathbf{g}}_{\mathrm{R}}^H\mathbf{X}_{1,i} & -\widetilde{\mathbf{g}}_{\mathrm{R}}^H\mathbf{X}_{1,i}\widetilde{\mathbf{g}}_{\mathrm{R}} - \sigma_{\mathrm{R}}^2 - \varpi_{1,i}\sum_{j\in\mathcal{S}} e_{\mathrm{R},j}^2 \end{bmatrix} \succeq \mathbf{0}, \\
&\qquad\qquad \varpi_{1,i} \ge 0, \\
&\begin{bmatrix} \varpi_{0,i}\mathbf{I} - \mathbf{X}_{0,i} & -\mathbf{X}_{0,i}\widetilde{\mathbf{g}}_{\mathrm{R}} \\ -\widetilde{\mathbf{g}}_{\mathrm{R}}^H\mathbf{X}_{0,i} & -\widetilde{\mathbf{g}}_{\mathrm{R}}^H\mathbf{X}_{0,i}\widetilde{\mathbf{g}}_{\mathrm{R}} - \sigma_{\mathrm{R}}^2 - \varpi_{0,i}\sum_{j\in\mathcal{S}} e_{\mathrm{R},j}^2 \end{bmatrix} \succeq \mathbf{0}, \\
&\qquad\qquad \varpi_{0,i} \ge 0, \forall i \in \mathcal{T},
\end{aligned} \tag{29}$$

where $\varpi_{1,i}$ and $\varpi_{0,i}$ are the introduced auxiliary variables. Now, we can rewrite (17) as

$$\max_{\mathbf{W}_k,\mathbf{R},\mathbf{F}_{1,i},\mathbf{F}_{0,i},\mu_k,\phi_i,\varpi_{1,i},\varpi_{0,i},t} \quad t \tag{30a}$$

$$\text{s.t.} \quad \mathrm{Tr}\left(\sum_{k\in\mathcal{K}}\mathbf{W}_k + \mathbf{R}\right) \le P, \tag{30b}$$

$$\mathrm{Tr}\left(\mathbf{F}_{1,i}\right) = 1, \mathrm{Tr}\left(\mathbf{F}_{0,i}\right) = 1, \forall i \in \mathcal{T}, \tag{30c}$$

$$\mathbf{W}_k \succeq \mathbf{0}, \forall k \in \mathcal{K}, \mathbf{R} \succeq \mathbf{0}, \tag{30d}$$

$$\mathbf{F}_{1,i} \succeq \mathbf{0}, \mathbf{F}_{0,i} \succeq \mathbf{0}, \forall i \in \mathcal{T}, \tag{30e}$$

$$\mathrm{Rank}\left(\mathbf{W}_k\right) = 1, \forall k \in \mathcal{K}, \tag{30f}$$

$$\mathrm{Rank}\left(\mathbf{F}_{1,i}\right) = 1, \mathrm{Rank}\left(\mathbf{F}_{0,i}\right) = 1, \forall i \in \mathcal{T}, \tag{30g}$$

$$(21), (22), (29). \tag{30h}$$

Omitting the non-convex rank-one constraints (30f) and (30g), the above problem is relaxed as

$$\begin{aligned}
\max_{\mathbf{W}_k,\mathbf{R},\mathbf{F}_{1,i},\mathbf{F}_{0,i},\mu_k,\phi_i,\varpi_{1,i},\varpi_{0,i},t} \quad & t \\
\text{s.t.} \quad & (21), (22), (29), (30b), (30c), (30d), (30e).
\end{aligned} \tag{31}$$

Problem (31) is still non-convex due to coupled transmit and receive variables, as well as the objective value t in $\mathbf{D}_{1,i}$ and $\mathbf{D}_{0,i}$. In the following, we propose an AO-based approach to solve this problem efficiently.

C. Proposed Transceiver Design Framework

Given the transmit (receive) variables and t, the sub-problem w.r.t. the receive (transmit) variables is a convex feasibility-checking SDP problem. Based on this property, we employ the AO framework to solve (31). Specifically, we optimize the transmit and receive variables in an alternate manner. Define the lower and upper bound of t as $\underline{t}$ and $\bar{t}$, respectively. In the l-th iteration, we first deal with the sub-problem w.r.t. the transmit variables while fixing the receive variables to the values of the last iteration, i.e., $\mathbf{F}_{1,i}^{(l-1)}$ and $\mathbf{F}_{0,i}^{(l-1)}, \forall i \in \mathcal{T}$. The convex feasibility-checking problem is formulated as

$$\text{find} \quad \mathbf{W}_k, \mathbf{R}, \mu_k, \phi_i, \varpi_{1,i}, \varpi_{0,i} \tag{32a}$$

$$\text{s.t. } t = t_{\mathrm{tx}}^{(l)}, \mathbf{F}_{1,i} = \mathbf{F}_{1,i}^{(l-1)}, \mathbf{F}_{0,i} = \mathbf{F}_{0,i}^{(l-1)}, \forall i \in \mathcal{T}, \tag{32b}$$

$$(21), (22), (29), (30b), (30d), \tag{32c}$$

where $t_{\mathrm{tx}}^{(l)}$ is the given objective value. The initial lower and upper bounds for $t_{\mathrm{tx}}^{(l)}$ are given by $\underline{t}_{\mathrm{tx}}^{(l)} = t^{(l-1)}$ and $\bar{t}_{\mathrm{tx}}^{(l)} = \bar{t}$, respectively, where $t^{(l-1)}$ is the objective value of the last iteration. Then, we try to improve $t_{\mathrm{tx}}^{(l)}$ by checking the feasibility of (32) iteratively. To be exact, in each inner loop, we update the objective value by $t_{\mathrm{tx}}^{(l)} = \frac{\underline{t}_{\mathrm{tx}}^{(l)} + \bar{t}_{\mathrm{tx}}^{(l)}}{2}$. If feasible, we update

$$\gamma_{1,i}^R = \frac{\mathrm{Vec}^H\left(\mathbf{H}_{\mathrm{R},i}\right)\left(\left(\sum_{k\in\mathcal{K}}\mathbf{W}_k + \mathbf{R}\right)^* \otimes \mathbf{F}_{1,i}\right)\mathrm{Vec}\left(\mathbf{H}_{\mathrm{R},i}\right)}{\sum_{j\in\mathcal{S}/i}\mathrm{Vec}^H\left(\mathbf{H}_{\mathrm{R},j}\right)\left(\left(\sum_{k\in\mathcal{K}}\mathbf{W}_k + \mathbf{R}\right)^* \otimes \mathbf{F}_{1,i}\right)\mathrm{Vec}\left(\mathbf{H}_{\mathrm{R},j}\right) + \sigma_{\mathrm{R}}^2}, \tag{24}$$

$$\gamma_{0,i}^R = \frac{\mathrm{Vec}^H\left(\mathbf{H}_{\mathrm{R},i}\right)\left(\left(\sum_{k\in\mathcal{K}_o}\mathbf{W}_k + \mathbf{R}\right)^* \otimes \mathbf{F}_{0,i}\right)\mathrm{Vec}\left(\mathbf{H}_{\mathrm{R},i}\right)}{\sum_{j\in\mathcal{S}/i}\mathrm{Vec}^H\left(\mathbf{H}_{\mathrm{R},j}\right)\left(\left(\sum_{k\in\mathcal{K}_o}\mathbf{W}_k + \mathbf{R}\right)^* \otimes \mathbf{F}_{0,i}\right)\mathrm{Vec}\left(\mathbf{H}_{\mathrm{R},j}\right) + \sigma_{\mathrm{R}}^2}, \tag{25}$$

the lower bound by $\underline{t}_{\text{tx}}^{(l)} = t_{\text{tx}}^{(l)}$, and store $\mathbf{W}_k^{(l)}, \forall k \in \mathcal{K}$, and $\mathbf{R}^{(l)}$. Otherwise, we update the upper bound by $\bar{t}_{\text{tx}}^{(l)} = t_{\text{tx}}^{(l)}$. We repeat this process until $\bar{t}_{\text{tx}}^{(l)} - \underline{t}_{\text{tx}}^{(l)} \leq \delta$, where δ is a predetermined tolerance. Then, we renew $t^{(l)} = t_{\text{tx}}^{(l)}$.

Similarly, for the subproblem w.r.t. the receive variables, we initialize the lower and upper bounds of the objective value as $\underline{t}_{\text{rx}}^{(l)} = t^{(l)}$ and $\bar{t}_{\text{rx}}^{(l)} = \bar{t}$. The corresponding convex feasibility-checking problem is given by

$$\text{find} \quad \mathbf{F}_{1,i}, \mathbf{F}_{0,i}, \varpi_{1,i}, \varpi_{0,i} \tag{33a}$$

$$\text{s.t.} \quad t = t_{\text{rx}}^{(l)}, \mathbf{W}_k = \mathbf{W}_k^{(l)}, \forall k \in \mathcal{K}, \tag{33b}$$

$$(29), (30c), (30e), \tag{33c}$$

where $t_{\text{rx}}^{(l)}$ is the given objective value. Again, $t_{\text{rx}}^{(l)}$, $\underline{t}_{\text{rx}}^{(l)}$, and $\bar{t}_{\text{rx}}^{(l)}$ are iteratively updated by the bisection approach until the convergence condition $\bar{t}_{\text{rx}}^{(l)} - \underline{t}_{\text{rx}}^{(l)} \leq \delta$ is met. Then, we renew $t^{(l)} = t_{\text{rx}}^{(l)}$, $\underline{t}_{\text{tx}}^{(l)} = t^{(l)}$, and $\bar{t}_{\text{tx}}^{(l)} = \bar{t}$, and enter the $(l+1)$-th iteration until the maximum iteration number L is reached. Note that the convergence of the algorithm could be theoretically guaranteed given sufficiently large L, as we analyze later. In fact, it usually takes no more than 4 outer iterations before the algorithm saturates, as we show in the numerical results.

To achieve convexity, the rank-one constraints (30f) and (30g) are omitted. Hence the output $\mathbf{W}_k$ and $\mathbf{F}_i$ from above steps may not be rank-one. To circumvent this problem, we integrate the rank-one constraints into the subproblems and propose a double-checked AO framework, i.e., ADC to make sure the rank-one property of corresponding transmit and receive variables in the following. To begin with, we present the following lemma [35] which can be used to lift the rank-one constraint into a more tractable matrix form.

Lemma 2: For a positive semi-definite Hermitian matrix $\mathbf{A} \in \mathbb{C}^{M\times M}$, the condition Rank $(\mathbf{A}) = 1$ is equivalent to the following conditions

$$\max_{\mathbf{B}} Tr(\mathbf{AB}) - 2v - Tr(\mathbf{V}) \geq 0, Tr(\mathbf{B}) = 1, \tag{34a}$$

$$\mathbf{V} - \mathbf{A} + v\mathbf{I}_M \succeq \mathbf{0}_M, \mathbf{B} \succeq \mathbf{0}_M, \mathbf{V} \succeq \mathbf{0}_M, \tag{34b}$$

where v and the Hermitian matrices $\mathbf{B}, \mathbf{V} \in \mathbb{C}^{M\times M}$ are the introduced auxiliary variables.

Incorporating constraint (30f) via Lemma 2, (32) is recast as

$$\text{find} \quad \mathbf{W}_k, \mathbf{R}, \mathbf{B}_k, \mathbf{V}_k, \mu_k, \phi_i, \varpi_{1,i}, \varpi_{0,i}, v_k \tag{35a}$$

$$\text{s.t.} \quad \text{Tr}(\mathbf{W}_k\mathbf{B}_k) - 2v_k - \text{Tr}(\mathbf{V}_k) \geq 0, \text{Tr}(\mathbf{B}_k) = 1, \tag{35b}$$

$$\mathbf{V}_k - \mathbf{W}_k + v_k\mathbf{I} \succeq \mathbf{0}, \mathbf{B}_k \succeq \mathbf{0}, \mathbf{V}_k \succeq \mathbf{0}, \forall k \in \mathcal{K}, \tag{35c}$$

$$(21), (22), (29), (30b), (30d), (32b), \tag{35d}$$

where v_k and $\mathbf{B}_k$, $\mathbf{V}_k \in \mathbb{C}^{M_t\times M_t}$ are the introduced auxiliary variables. During the inner loop w.r.t. the transmit variables, whenever (32) is feasible with $t_{\text{tx}}^{(l)}$, it is necessary to double-check if feasible transmit variables can also be found by (35) with the same $t_{\text{tx}}^{(l)}$. If not, we should not use $t_{\text{tx}}^{(l)}$ to update $\underline{t}_{\text{tx}}^{(l)}$ but $\bar{t}_{\text{tx}}^{(l)}$, i.e., to reduce the upper bound. Because transmit variables with rank-one property are not found even if (32) is feasible. Note that the only difficulty for double-checking is that (35) is non-convex due to the coupled $\mathbf{W}_k$ and $\mathbf{B}_k$ in constraint (35b). Nevertheless, we can overcome this difficulty in an iterative manner. Specifically, by fixing $\mathbf{W}_k$ in constraint (35b) to the value of the last loop, (35) becomes convex and can be solved to update $\mathbf{W}_k$ iteratively. If the value of $\mathbf{W}_k$ converges, i.e., the mean-square error of the values of two consecutive iterations is less than a given threshold τ in J iterations, the double-checking procedure is successful, and the corresponding rank-one transmit variables are found. Otherwise, the double-checking procedure fails, we should use $t_{\text{tx}}^{(l)}$ to update $\bar{t}_{\text{tx}}^{(l)}$ instead of $\underline{t}_{\text{tx}}^{(l)}$. The initial value of $\mathbf{W}_k$ is determined by the feasible solutions of (32) with $t_{\text{tx}}^{(l)}$.

Algorithm 1 Double-Checking for the Worst-Case Transmitter (Receiver) Design

Input: $\mathbf{F}_{1,i}^{(l-1)}$, $\mathbf{F}_{0,i}^{(l-1)}$, $\underline{t}_{\text{tx}}^{(l)}$, $\bar{t}_{\text{tx}}^{(l)}$ ($\mathbf{W}_k^{(l-1)}$, $\underline{t}_{\text{rx}}^{(l)}$, $\bar{t}_{\text{rx}}^{(l)}$), δ, τ, and J;
while $\bar{t}_{\text{tx}}^{(l)} - \underline{t}_{\text{tx}}^{(l)} > \delta$ ($\bar{t}_{\text{rx}}^{(l)} - \underline{t}_{\text{rx}}^{(l)} > \delta$) **do**
  Set $t_{\text{tx}}^{(l)} = (\underline{t}_{\text{tx}}^{(l)} + \bar{t}_{\text{tx}}^{(l)})/2$ ($t_{\text{rx}}^{(l)} = (\underline{t}_{\text{rx}}^{(l)} + \bar{t}_{\text{rx}}^{(l)})/2$);
  Let $\mathbf{F}_{1,i} = \mathbf{F}_{1,i}^{(l-1)}$, $\mathbf{F}_{0,i} = \mathbf{F}_{0,i}^{(l-1)}$, $t = t_{\text{tx}}^{(l)}$ ($\mathbf{W}_k = \mathbf{W}_k^{(l-1)}$, $\mathbf{R} = \mathbf{R}^{(l-1)}$, $t = t_{\text{rx}}^{(l)}$), and check the feasibility of (32) (check (33)).
  if feasible **then**
    Set $\mathbf{W}_k^{(l,0)} = \mathbf{W}_k^{(l)}$ ($\mathbf{F}_{1,i}^{(l,0)} = \mathbf{F}_{1,i}^{(l)}$ and $\mathbf{F}_{0,i}^{(l,0)} = \mathbf{F}_{0,i}^{(l)}$);
    for $j = 1 : J$ **do**
      Check the feasibility of (35) via setting $\mathbf{W}_k$ in (35b) as $\mathbf{W}_k^{(l,j-1)}$ ((36) via setting $\mathbf{F}_{1,i}$ in (36b) and $\mathbf{F}_{0,i}$ in (36d) as $\mathbf{F}_{1,i}^{(l,j-1)}$ and $\mathbf{F}_{0,i}^{(l,j-1)}$, respectively);
      if feasible **then**
        Store $\mathbf{W}_k^{(l,j)}$ ($\mathbf{F}_{1,i}^{(l,j)}$ and $\mathbf{F}_{0,i}^{(l,j)}$);
        if $\|\mathbf{W}_k^{(l,j)} - \mathbf{W}_k^{(l,j-1)}\| > \tau$ ($\|\mathbf{F}_{1,i}^{(l,j)} - \mathbf{F}_{1,i}^{(l,j-1)}\| > \tau$ or $\|\mathbf{F}_{0,i}^{(l,j)} - \mathbf{F}_{0,i}^{(l,j-1)}\| > \tau$) **then**
          Go to line 19;
        else
          Set $\underline{t}_{\text{tx}}^{(l)} = t_{\text{tx}}^{(l)}$ ($\underline{t}_{\text{rx}}^{(l)} = t_{\text{rx}}^{(l)}$) and break;
        end if
      else
        Set $\bar{t}_{\text{tx}}^{(l)} = t_{\text{tx}}^{(l)}$ ($\bar{t}_{\text{rx}}^{(l)} = t_{\text{rx}}^{(l)}$);
      end if
      $j = j + 1$;
    end for
    Set $\bar{t}_{\text{tx}}^{(l)} = t_{\text{tx}}^{(l)}$ ($\bar{t}_{\text{rx}}^{(l)} = t_{\text{rx}}^{(l)}$);
  else
    Set $\bar{t}_{\text{tx}}^{(l)} = t_{\text{tx}}^{(l)}$ ($\bar{t}_{\text{rx}}^{(l)} = t_{\text{rx}}^{(l)}$);
  end if
end while
Output $\mathbf{W}_k = \mathbf{W}_k^{(l)}$, $\mathbf{R} = \mathbf{R}^{(l)}$, $t_{\text{tx}}^{(l)}$ ($\mathbf{F}_{1,i} = \mathbf{F}_{1,i}^{(l)}$, $\mathbf{F}_{0,i} = \mathbf{F}_{0,i}^{(l)}$, $t_{\text{rx}}^{(l)}$).

Likewise, by incorporating constraint (30g), receiver-side problem (33) is transformed into

$$\text{find} \quad \mathbf{F}_{1,i}, \mathbf{F}_{0,i}, \mathbf{U}_{1,i}, \mathbf{U}_{0,i}, \mathbf{Z}_{1,i}, \mathbf{Z}_{0,i}, \varpi_{1,i}, \varpi_{0,i}, u_{1,i}, u_{0,i} \tag{36a}$$

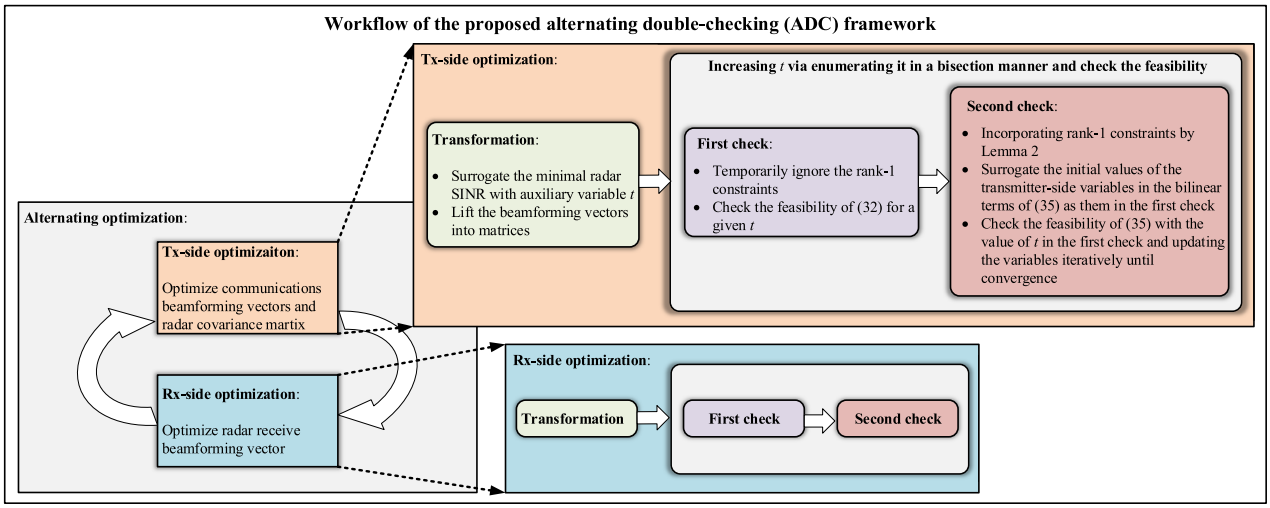

Fig. 2. The workflow of the proposed ADC framework.

$$\text{s.t.} \quad \mathrm{Tr}\left(\mathbf{F}_{1,i}\mathbf{U}_{1,i}\right) - 2u_{1,i} - \mathrm{Tr}\left(\mathbf{Z}_{1,i}\right) \geq 0, \mathrm{Tr}\left(\mathbf{U}_{1,i}\right) = 1, \tag{36b}$$

$$\mathbf{Z}_{1,i} - \mathbf{U}_{1,i} + u_{1,i}\mathbf{I} \succeq \mathbf{0}_{M_r}, \mathbf{U}_{1,i} \succeq \mathbf{0}, \mathbf{Z}_{1,i} \succeq \mathbf{0}, \tag{36c}$$

$$\mathrm{Tr}\left(\mathbf{F}_{0,i}\mathbf{U}_{0,i}\right) - 2u_{0,i} - \mathrm{Tr}\left(\mathbf{Z}_{0,i}\right) \geq 0, \mathrm{Tr}\left(\mathbf{U}_{0,i}\right) = 1, \tag{36d}$$

$$\mathbf{Z}_{0,i} - \mathbf{U}_{0,i} + u_{0,i}\mathbf{I} \succeq \mathbf{0}, \mathbf{U}_{0,i} \succeq \mathbf{0}, \mathbf{Z}_{0,i} \succeq \mathbf{0}, \forall i \in \mathcal{T}, \tag{36e}$$

$$(29), (30c), (30e), (33b), \tag{36f}$$

where $u_{1,i}$, $u_{0,i}$, and $\mathbf{U}_{1,i}, \mathbf{U}_{0,i}, \mathbf{Z}_{1,i}, \mathbf{Z}_{0,i} \in \mathbb{C}^{M_r \times M_r}$ are the introduced auxiliary variables. The receiver-side double-checking is similar to the transmitter-side one. We do not repeat it for brevity. Algorithm 1 details the steps of double-checking for both transmitter and receiver in parallel. Based on this, the robust scheme ADC for the worst-case transceiver design under bounded error model is summarized in Algorithm 2. The output transmit and receive variables $\mathbf{W}_k$, $\mathbf{F}_{1,i}$, and $\mathbf{F}_{0,i}$ are guaranteed to be rank-one. By simply using the eigenvalue decomposition (ED), we can get the corresponding optimized beamformers.

We illustrate the general structure of the proposed ADC framework in Fig. 2, outlining the key steps of transmitter-side optimization. Receiver-side details are omitted for brevity. It is worth noting that traditional Gaussian randomization [36] is not applicable to retrieve the rank-one property in the second check of the ADC framework for several reasons. Firstly, the numerous constraints within the problem, including communication and radar SINR requirements, as well as covertness constraints, make the likelihood of obtaining feasible rank-one matrices via Gaussian randomization exceedingly low. Secondly, the structure of the transmit waveform, consisting of beamformed data streams and a dedicated radar signal, results in a covariance matrix dependent on both beamformer-lifted matrices and the radar covariance matrix. However, Gaussian randomization solely generates beamformer-lifted matrices, leaving the radar covariance matrix unchanged, thus distorting the overall waveform structure and hindering the attainment of a feasible solution. Lastly, the iterative nature of the procedure, necessitated by the enumeration of each t, renders traditional Gaussian randomization highly time-consuming and unreliable for our purposes.

Algorithm 2 ADC for the Worst-Case Transceiver Design

1: **Input**: Initial receive variables $\mathbf{F}_{1,i}^{(0)}$ and $\mathbf{F}_{0,i}^{(0)}$, $\underline{t}$, $\bar{t}$, δ, L, τ, and J;
2: Set $l = 1$ and $t^{(0)} = \underline{t}$;
3: **for** $l \leq L$ **do**
4: Set $\underline{t}_{\mathrm{tx}}^{(l)} = t^{(l-1)}$ and $\bar{t}_{\mathrm{tx}}^{(l)} = \bar{t}$, optimize transmitter via the transmitter-side Algorithm 1;
5: Set $t^{(l)} = t_{\mathrm{tx}}^{(l)}$;
6: Set $\underline{t}_{\mathrm{rx}}^{(l)} = t^{(l)}$ and $\bar{t}_{\mathrm{rx}}^{(l)} = \bar{t}$, optimize receiver via the receiver-side Algorithm 1;
7: Set $t^{(l)} = t_{\mathrm{rx}}^{(l)}$ and $l = l + 1$;
8: **end for**
9: Output $\mathbf{W}_k = \mathbf{W}_k^{(l)}$, $\mathbf{R} = \mathbf{R}^{(L)}$, $\mathbf{F}_{1,i} = \mathbf{F}_{1,i}^{(L)}$, $\mathbf{F}_{0,i} = \mathbf{F}_{0,i}^{(L)}$, $t = t^{(L)}$.

We remark that the initial receive variables can be determined by $\mathbf{F}_{1,i}^{(0)} = \mathbf{I}_{M_r}/M_r$ and $\mathbf{F}_{0,i}^{(0)} = \mathbf{I}_{M_r}/M_r$. Moreover, the lower bound $\underline{t}$ should be chosen as a sufficiently small value such that (31) with $\mathbf{F}_{1,i} = \mathbf{F}_{1,i}^{(0)}$, $\mathbf{F}_{1,i} = \mathbf{F}_{1,i}^{(0)}, \forall i \in \mathcal{T}$, and $t = \underline{t}$ remains feasible. Otherwise, the optimization will fail because no feasible solutions can be found even in the first iteration of the inner loop concerning the transmit variables. Meanwhile, the upper bound $\bar{t}$ should be chosen as a sufficiently large value such that (31) is always infeasible at the first iteration of the inner loop w.r.t. both transmit and receive variables. Otherwise, the algorithm will end before reaching the stationary point. We further remark that although the feasible receive variables are not necessarily rank-one after the first check, simulations show that it is almost always the case. This indicates that most of the time we could obtain the

rank-one $\mathbf{F}_{1,i}$ and $\mathbf{F}_{0,i}$ directly without undergoing the second check.

IV. Outage-Constrained Robust Design Under Probabilistic Error Model

In practice, the worst-case design under bounded error model may be too strict and fails to capture the historical statistic of the CSI error [33]. To address this issue, in this section, we will focus on the probabilistic CSI error model and investigate the corresponding outage-constrained robust transceiver design. Similar to the worst-case design, in the following, we first formulate the problem and transform the SICs therein into convex LMIs and second-order cone constraints. Then, we leverage the AO framework to solve this problem.

A. Problem Formulation

The outage probabilities for radar SINR, communications SINR, and covertness constraint are defined as $\rho_{\mathrm{R},i}$, $\rho_{\mathrm{C},k}$, and $\rho_{\mathrm{W},i}$, respectively. Besides, as in the worst-case design, we lift the transmit and receive beamformers as matrices. The optimization problem to maximize the minimum outage-constrained radar SINR among all targets, denoted by t, is formulated as

$$\max_{\mathbf{W}_k,\mathbf{R},\mathbf{F}_{1,i},\mathbf{F}_{0,i},t} t \tag{37a}$$

$$\text{s.t.} \quad \Pr\left\{\gamma_{1,i}^R \geq t\right\} \geq 1-\rho_{\mathrm{R},i}, \Pr\left\{\gamma_{0,i}^R \geq t\right\} \geq 1-\rho_{\mathrm{R},i},$$

$$\Delta\mathbf{g}_{\mathrm{R}} \sim \mathcal{CN}\left(\mathbf{0}, \mathbf{E}_{\mathrm{R}}\right), \forall i \in \mathcal{T}, \tag{37b}$$

$$\Pr\left\{\gamma_{1,k}^C \geq \Gamma_k\right\} \geq 1-\rho_{\mathrm{C},k},$$

$$\Delta\mathbf{h}_{\mathrm{C},k} \sim \mathcal{CN}\left(\mathbf{0}, \mathbf{E}_{\mathrm{C},k}\right), \forall k \in \mathcal{K}, \tag{37c}$$

$$\Pr\{\ (14)\} \geq 1-\rho_{\mathrm{W},i},$$

$$\Delta\mathbf{h}_{\mathrm{W},i} \sim \mathcal{CN}\left(\mathbf{0}, \mathbf{E}_{\mathrm{W},i}\right), \forall i \in \mathcal{T}, \tag{37d}$$

$$(30b), (30c), (30d), (30e), (30f), (30g), \tag{37e}$$

where (37c) and (37d) denote the outage-constrained constraints for communications SINR and covertness of the system, respectively, and $\mathbf{E}_{\mathrm{R}} = \mathrm{Diag}(\mathbf{E}_{\mathrm{R},1}, \ldots, \mathbf{E}_{\mathrm{R},T+C}) \in \mathbb{C}^{(T+C)M_tM_r \times (T+C)M_tM_r}$. Due to the probabilistic errors, constraints (37b)-(37d) have no simple close-form expressions, which makes the above problem computationally prohibitive.

B. Problem Reformulation and Solving

To deal with constraints (37b)-(37d), we introduce the following useful lemma.

Lemma 3: (Bernstein-Type Inequality [33]): Given random variable $\mathbf{x} \sim \mathcal{CN}(\mathbf{0}, \mathbf{I}_M)$, $\mathbf{A} \in \mathbb{C}^{M\times M}$, $\mathbf{b} \in \mathbb{C}^{M\times 1}$, $s \in \mathbb{R}$, *and* $\rho \in [0,1]$. *The sufficient conditions for*

$$Pr\left\{\mathbf{x}^H\mathbf{A}\mathbf{x} + 2Re\left\{\mathbf{b}\mathbf{x}\right\} + s \geq 0\right\} \geq 1-\rho, \tag{38}$$

are presented in the following constraints

$$Tr\left(\mathbf{A}\right) - \sqrt{2\ln\left(\frac{1}{\rho}\right)}x + \ln\left(\rho\right)y + s \geq 0,$$
$$\sqrt{\left\|\mathbf{A}\right\|_F^2 + 2\left\|\mathbf{b}\right\|^2} \leq x, y\mathbf{I}_M + \mathbf{A} \succeq \mathbf{0}_M, y \geq 0, \tag{39}$$

where x *and* y *are the introduced auxiliary variables.*

We first handle the radar SINR constraints. Define $\Delta\widehat{\mathbf{g}}_{\mathrm{R}} = \mathbf{E}_{\mathrm{R}}^{-\frac{1}{2}}\Delta\mathbf{g}_{\mathrm{R}}$. Similar to the formulation of (26), the events presented in the probabilistic constraint (37b) can be transformed into

$$\begin{aligned}
&\Delta\widehat{\mathbf{g}}_{\mathrm{R}}^H\mathbf{E}_{\mathrm{R}}^{\frac{1}{2}}\mathbf{X}_{1,i}\mathbf{E}_{\mathrm{R}}^{\frac{1}{2}}\Delta\widehat{\mathbf{g}}_{\mathrm{R}} + 2\mathrm{Re}\left\{\left(\mathbf{E}_{\mathrm{R}}^{\frac{1}{2}}\mathbf{X}_{1,i}\widetilde{\mathbf{g}}_{\mathrm{R}}\right)^H\Delta\widehat{\mathbf{g}}_{\mathrm{R}}\right\} \\
&\quad + \widetilde{\mathbf{g}}_{\mathrm{R}}^H\mathbf{X}_{1,i}\widetilde{\mathbf{g}}_{\mathrm{R}} + \sigma_{\mathrm{R}}^2 \leq 0, \\
&\Delta\widehat{\mathbf{g}}_{\mathrm{R}}^H\mathbf{E}_{\mathrm{R}}^{\frac{1}{2}}\mathbf{X}_{0,i}\mathbf{E}_{\mathrm{R}}^{\frac{1}{2}}\Delta\widehat{\mathbf{g}}_{\mathrm{R}} + 2\mathrm{Re}\left\{\left(\mathbf{E}_{\mathrm{R}}^{\frac{1}{2}}\mathbf{X}_{0,i}\widetilde{\mathbf{g}}_{\mathrm{R}}\right)^H\Delta\widehat{\mathbf{g}}_{\mathrm{R}}\right\} \\
&\quad + \widetilde{\mathbf{g}}_{\mathrm{R}}^H\mathbf{X}_{0,i}\widetilde{\mathbf{g}}_{\mathrm{R}} + \sigma_{\mathrm{R}}^2 \leq 0, \Delta\widehat{\mathbf{g}}_{\mathrm{R}} \sim \mathcal{CN}\left(\mathbf{0}, \mathbf{I}\right), \forall i \in \mathcal{T}.
\end{aligned} \tag{40}$$

Subsequently, by Lemma 2, the sufficient conditions for constraint (37b) are given by

$$\begin{aligned}
&\mathrm{Tr}\left(\mathbf{E}_{\mathrm{R}}^{\frac{1}{2}}\mathbf{X}_{1,i}\mathbf{E}_{\mathrm{R}}^{\frac{1}{2}}\right) \\
&\quad + \sqrt{2\ln\left(\frac{1}{\rho_{\mathrm{R},i}}\right)}x_{1,i}^R - \ln\left(\rho_{\mathrm{R},i}\right)y_{1,i}^R \\
&\quad + \widetilde{\mathbf{g}}_{\mathrm{R}}^H\mathbf{X}_{1,i}\widetilde{\mathbf{g}}_{\mathrm{R}} + \sigma_{\mathrm{R}}^2 \leq 0, \\
&\sqrt{\left\|\mathbf{E}_{\mathrm{R}}^{\frac{1}{2}}\mathbf{X}_{1,i}\mathbf{E}_{\mathrm{R}}^{\frac{1}{2}}\right\|_{\mathrm{F}}^2 + 2\left\|\mathbf{E}_{\mathrm{R}}^{\frac{1}{2}}\mathbf{X}_{1,i}\widetilde{\mathbf{g}}_{\mathrm{R}}\right\|^2} \leq x_{1,i}^R, \\
&y_{1,i}^R\mathbf{I} + \mathbf{E}_{\mathrm{R}}^{\frac{1}{2}}\mathbf{X}_{1,i}\mathbf{E}_{\mathrm{R}}^{\frac{1}{2}} \succeq \mathbf{0}, y_{1,i}^R \geq 0, \\
&\mathrm{Tr}\left(\mathbf{E}_{\mathrm{R}}^{\frac{1}{2}}\mathbf{X}_{0,i}\mathbf{E}_{\mathrm{R}}^{\frac{1}{2}}\right) + \sqrt{2\ln\left(\frac{1}{\rho_{\mathrm{R},i}}\right)}x_{0,i}^R - \ln\left(\rho_{\mathrm{R},i}\right)y_{0,i}^R \\
&\quad + \widetilde{\mathbf{g}}_{\mathrm{R}}^H\mathbf{X}_{0,i}\widetilde{\mathbf{g}}_{\mathrm{R}} + \sigma_{\mathrm{R}}^2 \leq 0, \\
&\sqrt{\left\|\mathbf{E}_{\mathrm{R}}^{\frac{1}{2}}\mathbf{X}_{0,i}\mathbf{E}_{\mathrm{R}}^{\frac{1}{2}}\right\|_{\mathrm{F}}^2 + 2\left\|\mathbf{E}_{\mathrm{R}}^{\frac{1}{2}}\mathbf{X}_{0,i}\widetilde{\mathbf{g}}_{\mathrm{R}}\right\|^2} \leq x_{0,i}^R, \\
&y_{0,i}^R\mathbf{I} + \mathbf{E}_{\mathrm{R}}^{\frac{1}{2}}\mathbf{X}_{0,i}\mathbf{E}_{\mathrm{R}}^{\frac{1}{2}} \succeq \mathbf{0}, y_{0,i}^R \geq 0, \forall i \in \mathcal{T},
\end{aligned} \tag{41}$$

where $x_{1,i}^R$, $x_{0,i}^R$, $y_{1,i}^R$, and $y_{0,i}^R$ are the introduced auxiliary variables.

Likewise, let $\Delta\widehat{\mathbf{g}}_{\mathrm{C},k} = \mathbf{E}_{\mathrm{C},k}^{-\frac{1}{2}}\Delta\mathbf{g}_{\mathrm{C},k}$. The sufficient conditions for the communications SINR constraint (37c) are expressed as

$$\begin{aligned}
&\mathrm{Tr}\left(\mathbf{E}_{\mathrm{C},k}^{\frac{1}{2}}\mathbf{\Psi}_k\mathbf{E}_{\mathrm{C},k}^{\frac{1}{2}}\right) - \sqrt{2\ln\left(\frac{1}{\rho_{\mathrm{C},k}}\right)}x_k^C + \ln\left(\rho_{\mathrm{C},k}\right)y_k^C \\
&\quad + \widetilde{\mathbf{h}}_{\mathrm{C},k}^H\mathbf{\Psi}_k\widetilde{\mathbf{h}}_{\mathrm{C},k} - \Gamma_k\sigma_{\mathrm{C},k}^2 \geq 0, \\
&\sqrt{\left\|\mathbf{E}_{\mathrm{C},k}^{\frac{1}{2}}\mathbf{\Psi}_k\mathbf{E}_{\mathrm{C},k}^{\frac{1}{2}}\right\|_{\mathrm{F}}^2 + 2\left\|\mathbf{E}_{\mathrm{C},k}^{\frac{1}{2}}\mathbf{\Psi}_k\widetilde{\mathbf{h}}_{\mathrm{C},k}\right\|^2} \leq x_k^C, \\
&y_k^C\mathbf{I} + \mathbf{E}_{\mathrm{C},k}^{\frac{1}{2}}\mathbf{\Psi}_k\mathbf{E}_{\mathrm{C},k}^{\frac{1}{2}} \succeq \mathbf{0}, y_k^C \geq 0, \forall k \in \mathcal{K},
\end{aligned} \tag{42}$$

where x_k^C and y_k^C are the introduced auxiliary variables.

For the probabilistic covertness constraint (37d), we define $\Delta\widehat{\mathbf{h}}_{\mathrm{W},i} = \mathbf{E}_{\mathrm{W},i}^{-\frac{1}{2}}\Delta\mathbf{h}_{\mathrm{W},i}, \forall i \in \mathcal{T}$ such that

TABLE II
ARITHMETIC COMPLEXITIES OF PROPOSED DESIGNS

Proposed ADC designs		Arithmetic complexity	
		Transmitter side	Receiver side
Algorithm 2	First check	$\mathcal{O}\left(\left(\left(K_o+K_c+1\right)M_t^2+K_o+K_c+4T\right)^{3.5}\right)$	$\mathcal{O}\left(\left(2TM_r^2+2T\right)^{3.5}\right)$
	Second check	$\mathcal{O}\left(\left(\left(3K_o+3K_c+1\right)M_t^2+2K_o+2K_c+4T\right)^{3.5}\right)$	$\mathcal{O}\left(\left(6TM_r^2+4T\right)^{3.5}\right)$
Algorithm 3	First check	$\mathcal{O}\left(\left(\left(K_o+K_c+1\right)M_t^2+2K_o+2K_c+8T\right)^{3.5}\right)$	$\mathcal{O}\left(\left(2TM_r^2+4T\right)^{3.5}\right)$
	Second check	$\mathcal{O}\left(\left(\left(3K_o+3K_c+1\right)M_t^2+3K_o+3K_c+8T\right)^{3.5}\right)$	$\mathcal{O}\left(\left(6TM_r^2+6T\right)^{3.5}\right)$

$\Delta\widehat{\mathbf{h}}_{\mathrm{W},i} \sim \mathcal{CN}\left(\mathbf{0},\mathbf{I}_{M_t}\right)$. Similarly, the sufficient conditions are presented as

$$\begin{aligned}
&\mathrm{Tr}\left(-\mathbf{E}_{\mathrm{W},i}^{\frac{1}{2}}\boldsymbol{\Xi}\mathbf{E}_{\mathrm{W},i}^{\frac{1}{2}}\right)-\sqrt{2\ln\left(\frac{1}{\rho_{\mathrm{W},i}}\right)}x_i+\ln\left(\rho_{\mathrm{W},i}\right)y_i\\
&\quad+\eta\sigma_{\mathrm{W},i}^2-\widetilde{\mathbf{h}}_{\mathrm{W},i}^H\boldsymbol{\Xi}\widetilde{\mathbf{h}}_{\mathrm{W},i}\geq 0,\\
&\sqrt{\left\|\mathbf{E}_{\mathrm{W},i}^{\frac{1}{2}}\boldsymbol{\Xi}\mathbf{E}_{\mathrm{W},i}^{\frac{1}{2}}\right\|_{\mathrm{F}}^2+2\left\|\mathbf{E}_{\mathrm{W},i}^{\frac{1}{2}}\boldsymbol{\Xi}\widetilde{\mathbf{h}}_{\mathrm{W},i}\right\|^2}\leq x_i,\\
&y_i\mathbf{I}-\mathbf{E}_{\mathrm{W},i}^{\frac{1}{2}}\boldsymbol{\Xi}\mathbf{E}_{\mathrm{W},i}^{\frac{1}{2}}\succeq\mathbf{0},y_i\geq 0,\forall i\in\mathcal{T},
\end{aligned}\tag{43}$$

where x_i and y_i are the introduced auxiliary variables.

Above all, by omitting the rank-one constraints (30f) and (30g), (37) is transformed into the following problem

$$\begin{aligned}
&\max_{\mathbf{W}_k,\mathbf{R},\mathbf{F}_{1,i},\mathbf{F}_{0,i},x_k^C,y_k^C,x_{1,i}^R,x_{0,i}^R,y_{1,i}^R,y_{0,i}^R,x_i,y_i,t}\quad t\\
&\text{s.t. (41), (42), (43), (30}b\text{), (30}c\text{), (30}d\text{), (30}e\text{).}
\end{aligned}\tag{44}$$

Similar to (31), (44) is still non-convex due to the coupled transmit and receive variables as well as the objective value t. Besides, (44) is also a convex feasibility-checking problem with given transmit (receive) variables and t. By straightforwardly formulating the corresponding transmitter and receiver-side feasibility-checking subproblems, the AO-based double-checking framework as in Algorithm 2 can be readily used to solve the outage-constrained transceiver design under probabilistic error model. To avoid redundancy, we do not repeat the detailed steps and directly refer to them as Algorithm 3 which outputs the optimized radar covariance matrix $\mathbf{R}$, and the rank-one transmit and receive variables $\mathbf{W}_k$, $\mathbf{F}_{1,i}$, and $\mathbf{F}_{0,i}$. Then, we further utilize ED to obtain high-quality transmit and beamformers.

The convergence of the proposed designs are determined by the AO-based algorithms. We only need to show the convergence of Algorithm 2. The convergence of Algorithm 3 can be verified in the same manner. For notational convenience, we denote the transmit and receive variables as $\mathbf{W}=[\mathbf{W}_1,\ldots,\mathbf{W}_k,\mathbf{R}]$ and $\mathbf{F}=[\mathbf{F}_{1,1},\ldots,\mathbf{F}_{1,T},\mathbf{F}_{0,1},\ldots,\mathbf{F}_{0,T}]$, respectively. Then, the objective value t can be regarded as a function w.r.t. $\mathbf{W}$ and $\mathbf{F}$, i.e., $t(\mathbf{W},\mathbf{F})$. In each iteration of Algorithm 2, the objective value is updated sequentially by the loops w.r.t. $\mathbf{W}^{(l)}$ and $\mathbf{F}^{(l)}$, respectively. In particular, for a given $\mathbf{F}^{(l-1)}$, any $t^{(l)}$ enumerated by bisection with double-checked feasible $\mathbf{W}^{(l)}$ is greater than the initial value of $t^{(l)}$ in this transmitter-side loop. For a given $\mathbf{W}^{(l)}$, any $t^{(l)}$ enumerated by bisection with double-checked feasible $\mathbf{F}^{(l)}$ is greater than the initial value of $t^{(l)}$ in this receiver-side loop. Hence we have $t(\mathbf{W}^{(l-1)},\mathbf{F}^{(l-1)})\leq t(\mathbf{W}^{(l)},\mathbf{F}^{(l-1)})\leq t(\mathbf{W}^{(l)},\mathbf{F}^{(l)})$. We notice that $t(\mathbf{W}^{(l)},\mathbf{F}^{(l)})$ is upper-bounded by $\bar{t}$. As a result, the convergence of Algorithm 2 can be guaranteed. Moreover, as $l\rightarrow+\infty$, it can be shown that Algorithm 2 converges to a stationary point of (31) [37].

The arithmetic complexities of the proposed ADC designs consist of the complexities of the first and second checks of the transmitter and receiver-side designs, respectively. We present the component-wise complexities for both Algorithms 2 and 3 in Table II. Let $C_{1,\mathrm{tx}}$, $C_{2,\mathrm{tx}}$, $C_{1,\mathrm{rx}}$, and $C_{2,\mathrm{rx}}$ denote the complexities of the first and second checks of the transmitter and receiver-side designs. The worst-case overall complexity of each algorithm can be determined by $l_{\mathrm{tx}}(C_{1,\mathrm{tx}}+JC_{2,\mathrm{tx}})+l_{\mathrm{rx}}(C_{1,\mathrm{rx}}+JC_{2,\mathrm{rx}})$, where l_{tx} and l_{rx} denote the corresponding transmitter and receiver-side loop numbers, respectively.

V. NUMERICAL RESULTS

In this section, we present the numerical results to evaluate the performance of the proposed algorithms for the covert ISAC system. Unless specified otherwise, the basic simulation parameters are set as follows. The ISAC BS is equipped with $M_t=6$ transmit antennas and $M_r=6$ receive antennas with half-wavelength interval. The power budget of the BS is set as $P=30$dBm. There are $T=2$ targets located at 80° and 100°, respectively, and $C=2$ clutters located at 40° and 150°, respectively. Each of the radar channel coefficients are given by $\alpha_j=0$dB and $\beta_i=0$dB. Besides, the BS serves $K_o=2$ overt users and $K_c=2$ covert users. Each communications channel is assumed to be Rayleigh fading and $\mathbf{h}_{\mathrm{C},k}\sim\mathcal{CN}\left(\mathbf{0}_{M_t},\mathbf{I}_{M_t}\right)$. The noise powers are set as $\sigma_{\mathrm{W},i}^2=0$dBm, $\sigma_{\mathrm{C},k}^2=0$dBm, and $\sigma_{\mathrm{R}}^2=0$dBm. The blocklength is set as $N=1000$ while the covertness constant is set as $\epsilon=0.1$. The overt and covert communications SINRs are set as $\Gamma_1=\Gamma_2=2$dB and $\Gamma_3=\Gamma_4=2$dB, respectively. The outage probabilities are set as $\rho_{\mathrm{R},1}\ldots=\rho_{\mathrm{R},1}=\rho_{\mathrm{R}}=0.05$, $\rho_{\mathrm{W},i}=0.05$, $\rho_{\mathrm{C},k}=0.05$. The CSI uncertainty is controlled by a coefficient given by $\kappa=0.01$. To present a fair comparison between the worst-case and outage-constrained designs, we follow the settings in [34]. For the probabilistic error model, we set $\mathbf{E}_{\mathrm{C},k}=\kappa\|\widetilde{\mathbf{h}}_{\mathrm{C},k}\|^2\mathbf{I}_{M_t}/M_t$, $\mathbf{E}_{\mathrm{W},i}=\kappa\|\widetilde{\mathbf{h}}_{\mathrm{W},i}\|^2\mathbf{I}_{M_t}/M_t$, and $\mathbf{E}_{\mathrm{R}}=\kappa\|\widetilde{\mathbf{g}}_{\mathrm{R}}\|^2\mathbf{I}_{(T+C)M_tM_r}/((T+C)M_tM_r)$, respectively. Accordingly, for the bounded error model, we set $e_{\mathrm{C},k}^2=\frac{\kappa\|\widetilde{\mathbf{h}}_{\mathrm{C},k}\|^2}{2}F_{\chi_{2M_t}^2}^{-1}\left(1-\rho_{\mathrm{C},k}\right)$, $e_{\mathrm{W},i}^2=\frac{\kappa\|\widetilde{\mathbf{h}}_{\mathrm{W},i}\|^2}{2}F_{\chi_{2M_t}^2}^{-1}\left(1-\rho_{\mathrm{W},i}\right)$, and $e_{\mathrm{R}}^2=\frac{\kappa\|\widetilde{\mathbf{g}}_{\mathrm{R}}\|^2}{2}F_{\chi_{2(T+C)M_tM_r}^2}^{-1}\left(1-\rho_{\mathrm{R}}\right)$, respectively. For conciseness, in the following figures, results obtained via

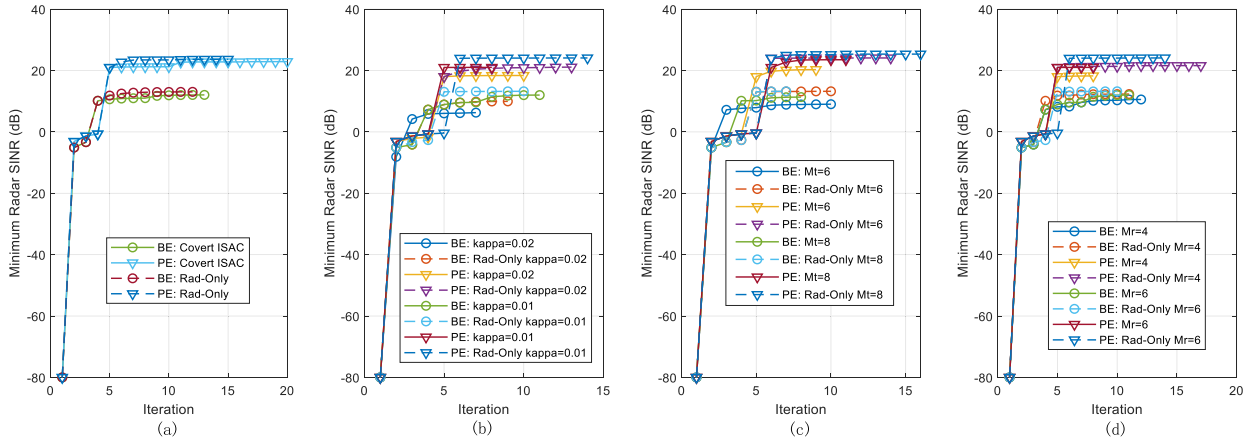

Fig. 3. Illustration of algorithmic convergence. (a) Comparison between the considered covert ISAC system and the radar-only upper bound. (b) Different uncertainty coefficients. (c) Different transmit antenna numbers. (d) Different receive antenna numbers.

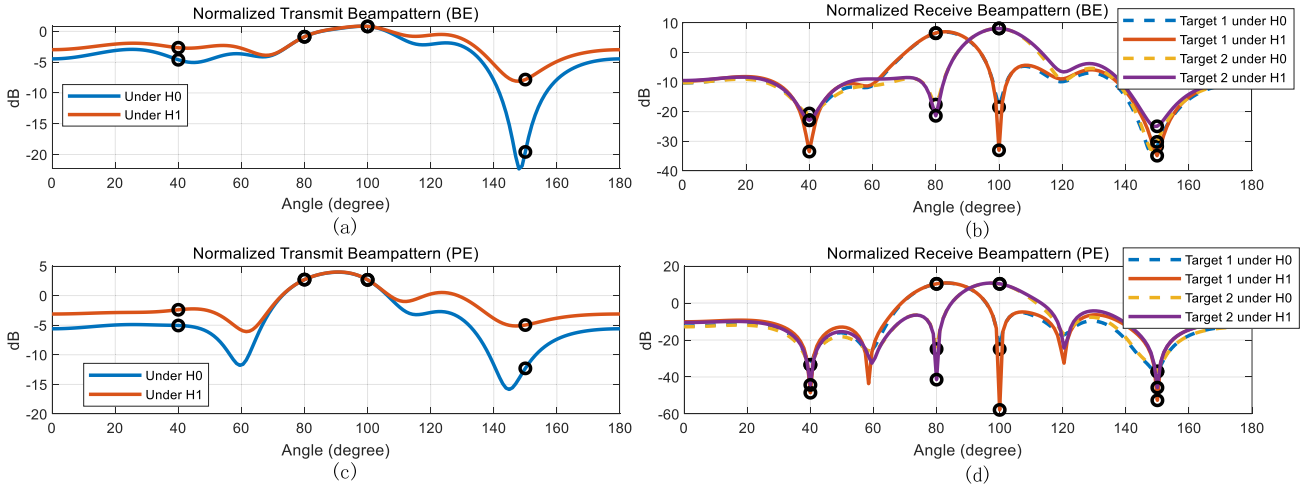

Fig. 4. Beampatterns. (a) Transmit beampattern under BE. (a) Receive beampattern under BE. (c) Transmit beampattern under PE. (d) Receive beampattern under PE.

Algo. 2 under bounded error model and via Algo. 3 under probabilistic error model are referred as results under BE and PE, respectively.

Figures 3(a)-(d) depict the convergence trends of the proposed algorithms compared to their radar-only upper bounds for different uncertainty coefficients and transmit/receive antenna numbers. The iteration number accumulates both the transmitter and receiver-side iteration. We can see that, all of them under different parametric configurations converge very fast. The huge boost in radar SINR observed within the first two iterations arises from the utilization of a very small initial value $\underline{t}$, which is intended to ensure the initial feasibility of the proposed ADC framework. Furthermore, for both results under BE and PE, less than 3 transmitter-receiver cycles of the proposed ADC framework are needed for the algorithms to converge to the stationary points regardless of the different antenna numbers and channel uncertainties. The radar SINR can be boosted significantly within the first two iterations. Meanwhile, higher radar SINR is obtained with less CSI uncertainty and more transmit and receive antennas, i.e., less systematic inaccuracy and more spatial DoFs. As validated in Figs. 3(a)-(d) and also in following simulations, owing to more conservative constraints, the worst-case design under BE leads to lower radar SINR than the outage-constrained counterpart under PE.

Figures 4(a)-(d) illustrates the transmit and receive beampatterns under both $\mathcal{H}_1$ and $\mathcal{H}_0$. In these subfigures, Figs. 4(a) and (b) are the transmit and receive beampatterns under BE, respectively, while Figs. 4(c) and (d) are the transmit and receive beampatterns under PE, respectively. As can be seen, in two phases, the transmit beampatterns do not necessarily have good resolutions towards the directions of the targets. However, after the receive beamforming, the receive powers at the directions of the targets are substantially boosted while those of the clutters are deeply nulled. In addition, for the receive beamforming w.r.t. target 1, the direction w.r.t. target 2 is also nulled and vice versa. As a result, the radar SINRs for both targets can be significantly improved after the receive beamforming of the proposed algorithms. The insight here is that it is not necessary to approximate the ideal transmit beampattern, as in [7], [8], [9], [10], and [11], to obtain desirable radar performance. This is because transmit beampattern is just an transmitter-side intermediate result instead of the overall measurement for radar performance. The

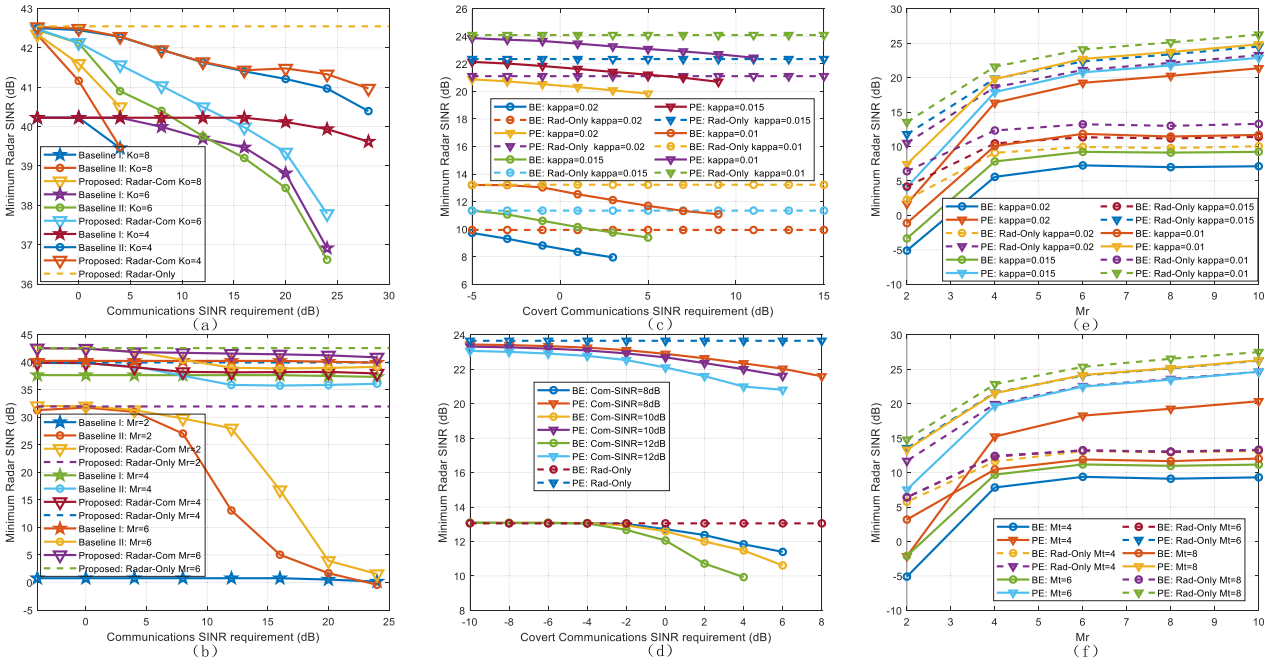

Fig. 5. (a) and (b) are the minimum radar SINR versus communications SINR requirement with perfect CSI for different overt user numbers and receive antenna numbers, respectively. (c) and (d) are the minimum radar SINR versus covert communications SINR for different uncertainty coefficients and overt communications SINRs, respectively. (e) and (f) are the minimum radar SINR versus receive antenna numbers for different uncertainty coefficients and transmit antenna numbers, respectively.

transmitter-side-only designs fail to exploit the receiver-side potentials to further enhance the radar performance.

To showcase the efficacy and versatility of the ISAC transceiver design framework, we evaluate its performance in the overt communications-only scenario with perfect CSI. In Figs. 5(a) and (b), we present the results of applying the proposed scheme and compare the minimum radar SINR with two state-of-the-art baselines [9], [20], both designed specifically for scenarios with perfect CSI. The design goals for [9] (Baseline I) and [20] (Baseline II) are summarized as minimizing the mean square error of the MIMO radar beampattern and maximizing the minimum radar SINR with receive beamforming matching the steering vector of the receive antenna array, respectively. Figures 5(a) and (b) demonstrate that our approach significantly outperforms the two baselines, especially when the communications SINR is relatively high, the number of served users are relatively large, and the receiver antenna numbers are relatively small. The reason for this is that our scheme fully exploits the ISAC transceiver by alternately designing the transmitter and receiver while Baseline I ignored the receiver-side design and Baseline II did not design the radar receiver adaptively.

To facilitate a comprehensive comparison between the proposed approach and baselines, we analyze their computational complexity as follows. Without the requirement of an iterative procedure, the overall complexity of Baseline I is at the same order as the complexity of Baseline II in each iteration. In the evaluated perfect CSI scenario with the absence of covert users, the transmitter-side design of the proposed ADC framework degenerates to that of Baseline II. Therefore, the complexity of Baseline II is at the same order as the complexity of the transmitter-side design of the proposed framework. As proved in [20], closed-form beamformers can be constructed after the first check, thus skipping the second check. Consequently, in the evaluated scenario, the complexities of Baseline I, Baseline II, and the proposed framework are denoted as $C_{1,\mathrm{tx}}$, $l_{\mathrm{tx}}C_{1,\mathrm{tx}}$, and $l_{\mathrm{tx}}C_{1,\mathrm{tx}} + l_{\mathrm{rx}}C_{1,\mathrm{rx}}$, respectively. As can be seen, the proposed scheme has the highest complexity due to its alternating nature. The complexity of Baseline II, which requires iterative optimization of the transmitter, is listed second, while Baseline I has the least complexity as no iterative procedure is included. However, as validated by Figs. 5(a) and (b), the cost of complexity is translated into the advantage of performance. The proposed scheme achieves the highest objective value, followed by Baseline II and Baseline I, in reverse order as the complexity.

Figures 5(c) and (d) plot the minimum radar SINR versus the covert communications SINR for different uncertainty coefficient κ and overt communications SINRs, respectively. In Fig. 5(c), it is evident that as κ increases, the radar SINR decreases for a given covert communications SINR. This phenomenon occurs due to the challenges posed by CSI errors in accurately directing beamforming towards radar targets. Moreover, with CSI errors, fulfilling QoS in terms of communication SINR and system covertness becomes more difficult. The escalating uncertainty in CSI necessitates the allocation of more resources by the BS to mitigate this inaccuracy. As a result, the resources available for radar sensing gradually diminish.

In Fig. 5(d), the decrease in maximum covert communications SINR alongside an increase in overt communications SINR offers valuable insights into the system's ability to balance radar, overt communications, and covert communications

performance. This trend highlights the inherent tripartite trade-off in the covert ISAC system, where improvements in one aspect inevitably lead to compromises in the other two. Specifically, as the covert communications SINR requirement rises, there's a corresponding decline in radar SINR for both design types. Furthermore, at a given level of radar SINR, the maximum covert communications SINR diminishes with higher overt communications SINR. These findings underscore the intricate interplay between the three functionalities of the system.

Fig. 5(d) also shows that when the covert communications SINR is sufficiently low, the minimum radar SINR of the covert ISAC system can approach that of a system dedicated solely to MIMO radar operations. This phenomenon arises from the transmitted waveform comprising both communications and dedicated radar waveforms, providing sufficient degrees of freedom to approximate the ideal radar-only covariance. This effect is particularly pronounced when the communications performance requirements are not stringent.

Figures 5(e) and (f) show the minimum radar SINR versus the receive antenna number M_r with different coefficient κ and the transmit antenna number M_t, respectively. As the number of receive antennas increases, it becomes evident that the radar SINR gain diminishes. This occurs because the receive antenna number ceases to be the predominant limiting factor for radar performance. In practice, it is crucial to judiciously determine the antenna number to strike a balance between performance and hardware cost, considering that algorithmic complexity scales proportionally with the number of antennas. From Fig. 5(e), we can observe that the uncertainty worsens the radar performance. For a given M_r, the radar SINR decreases as κ becomes larger, which is in line with the findings in Fig. 5(c). From Fig. 5(f), we can see that for a given M_r, the radar SINR increases as M_t becomes larger. In addition, the radar performance gap between the different transmit antenna numbers will shrink as M_r becomes larger. This is because the receiver-side DoFs can compensate for the insufficient transmitter-side DoFs, which further highlights the importance of receive beamforming design in covert ISAC systems.

VI. Conclusion

In this paper, we presented an optimization framework for the robust transceiver design in a covert ISAC system under imperfect CSI. Our approach balanced radar performance, communications requirements, and covertness of the system in the face of challenging non-convex optimization problems involving SICs and coupled beamformers. To overcome these issues, we introduced the S-procedure, Bernstein-type inequality, and ADC robust optimization framework to facilitate feasibility checking and optimization of the transmit and receive beamformers. Numerical results revealed the superiority of the proposed ISAC transceiver design framework, compared to the state-of-the-art designs, and demonstrated its robustness. Moreover, the significance of exploiting the receiver-side potentials on enhancing the performance of covert ISAC systems was highlighted.

Although the developed framework for ISAC transceivers has partially addressed the challenges of balancing radar performance, communication SINR, and system covertness, it is limited by its high computational complexity, stemming from the alternating nature and the involvement of solving SDP problems. Future research can focus on developing more efficient optimization algorithms to enhance feasibility and scalability, facilitating real-world deployment.

When multiple targets share a similar direction, the spatial overlap causes significant interference, leading to reduced system performance. Increasing system bandwidth can potentially solve this by enhancing range resolution, allowing the radar to distinguish targets and reduce interference. While our current analysis relies on a narrow-band model, investigating wideband models such as orthogonal frequency division multiplexing systems deserves further study.

References

[1] Y. Zhang, W. Ni, W. Tang, Y. C. Eldar, and D. Niyato, "Robust transceiver design for ISAC with imperfect CSI," in *Proc. IEEE Global Commun. Conf.*, Dec. 2023, pp. 1320–1325.

[2] F. Liu et al., "Integrated sensing and communications: Toward dual-functional wireless networks for 6G and beyond," *IEEE J. Sel. Areas Commun.*, vol. 40, no. 6, pp. 1728–1767, Jun. 2022.

[3] A. Hassanien, M. G. Amin, Y. D. Zhang, and F. Ahmad, "Dual-function radar-communications: Information embedding using sidelobe control and waveform diversity," *IEEE Trans. Signal Process.*, vol. 64, no. 8, pp. 2168–2181, Apr. 2016.

[4] T. Huang, N. Shlezinger, X. Xu, Y. Liu, and Y. C. Eldar, "MAJoR-Com: A dual-function radar communication system using index modulation," *IEEE Trans. Signal Process.*, vol. 68, pp. 3423–3438, 2020.

[5] C. Sturm and W. Wiesbeck, "Waveform design and signal processing aspects for fusion of wireless communications and radar sensing," *Proc. IEEE*, vol. 99, no. 7, pp. 1236–1259, Jul. 2011.

[6] Y. Huang, S. Hu, S. Ma, Z. Liu, and M. Xiao, "Designing low-PAPR waveform for OFDM-based RadCom systems," *IEEE Trans. Wireless Commun.*, vol. 21, no. 9, pp. 6979–6993, Sep. 2022.

[7] F. Liu, C. Masouros, A. Li, H. Sun, and L. Hanzo, "MU-MIMO communications with MIMO radar: From co-existence to joint transmission," *IEEE Trans. Wireless Commun.*, vol. 17, no. 4, pp. 2755–2770, Apr. 2018.

[8] F. Liu, L. Zhou, C. Masouros, A. Li, W. Luo, and A. Petropulu, "Toward dual-functional radar-communication systems: Optimal waveform design," *IEEE Trans. Signal Process.*, vol. 66, no. 16, pp. 4264–4279, Aug. 2018.

[9] X. Liu, T. Huang, N. Shlezinger, Y. Liu, J. Zhou, and Y. C. Eldar, "Joint transmit beamforming for multiuser MIMO communications and MIMO radar," *IEEE Trans. Signal Process.*, vol. 68, pp. 3929–3944, 2020.

[10] R. Liu, M. Li, Q. Liu, and A. L. Swindlehurst, "Dual-functional radar-communication waveform design: A symbol-level precoding approach," *IEEE J. Sel. Topics Signal Process.*, vol. 15, no. 6, pp. 1316–1331, Nov. 2021.

[11] X. Liu, T. Huang, and Y. Liu, "Transmit design for joint MIMO radar and multiuser communications with transmit covariance constraint," *IEEE J. Sel. Areas Commun.*, vol. 40, no. 6, pp. 1932–1950, Jun. 2022.

[12] F. Liu, Y.-F. Liu, A. Li, C. Masouros, and Y. C. Eldar, "Cramér–Rao bound optimization for joint radar-communication beamforming," *IEEE Trans. Signal Process.*, vol. 70, pp. 240–253, 2022.

[13] C. G. Tsinos, A. Arora, S. Chatzinotas, and B. Ottersten, "Joint transmit waveform and receive filter design for dual-function radar-communication systems," *IEEE J. Sel. Topics Signal Process.*, vol. 15, no. 6, pp. 1378–1392, Nov. 2021.

[14] R. Liu, M. Li, Q. Liu, and A. L. Swindlehurst, "Joint waveform and filter designs for STAP-SLP-based MIMO-DFRC systems," *IEEE J. Sel. Areas Commun.*, vol. 40, no. 6, pp. 1918–1931, Jun. 2022.

[15] L. Chen, Z. Wang, Y. Du, Y. Chen, and F. R. Yu, "Generalized transceiver beamforming for DFRC with MIMO radar and MU-MIMO communication," *IEEE J. Sel. Areas Commun.*, vol. 40, no. 6, pp. 1795–1808, Jun. 2022.

[16] Y. Li and M. Jiang, "Joint transmit beamforming and receive filters design for coordinated two-cell interfering dual-functional radar-communication networks," *IEEE Trans. Veh. Technol.*, vol. 71, no. 11, pp. 12362–12367, Nov. 2022.

[17] B. Tang and P. Stoica, "MIMO multifunction RF systems: Detection performance and waveform design," *IEEE Trans. Signal Process.*, vol. 70, pp. 4381–4394, 2022.

[18] N. Zhao, Y. Wang, Z. Zhang, Q. Chang, and Y. Shen, "Joint transmit and receive beamforming design for integrated sensing and communication," *IEEE Commun. Lett.*, vol. 26, no. 3, pp. 662–666, Mar. 2022.

[19] Y. Ni, Z. Wang, and Q. Huang, "Joint transceiver beamforming for multi-target single-user joint radar and communication," *IEEE Wireless Commun. Lett.*, vol. 11, no. 11, pp. 2360–2364, Nov. 2022.

[20] J. Pritzker, J. Ward, and Y. C. Eldar, "Transmit precoder design approaches for dual-function radar-communication systems," 2022, *arXiv:2203.09571*.

[21] C. Wen, Y. Huang, and T. N. Davidson, "Efficient transceiver design for MIMO dual-function radar-communication systems," *IEEE Trans. Signal Process.*, vol. 71, pp. 1786–1801, 2023.

[22] S. Ma et al., "Covert beamforming design for integrated radar sensing and communication systems," *IEEE Trans. Wireless Commun.*, vol. 22, no. 1, pp. 718–731, Jan. 2023.

[23] A. Deligiannis, A. Daniyan, S. Lambotharan, and J. A. Chambers, "Secrecy rate optimizations for MIMO communication radar," *IEEE Trans. Aerosp. Electron. Syst.*, vol. 54, no. 5, pp. 2481–2492, Oct. 2018.

[24] P. Liu, Z. Fei, X. Wang, B. Li, Y. Huang, and Z. Zhang, "Outage constrained robust secure beamforming in integrated sensing and communication systems," *IEEE Wireless Commun. Lett.*, vol. 11, no. 11, pp. 2260–2264, Nov. 2022.

[25] N. Su, F. Liu, and C. Masouros, "Secure radar-communication systems with malicious targets: Integrating radar, communications and jamming functionalities," *IEEE Trans. Wireless Commun.*, vol. 20, no. 1, pp. 83–95, Jan. 2021.

[26] X. Wang, Z. Fei, J. A. Zhang, and J. Huang, "Sensing-assisted secure uplink communications with full-duplex base station," *IEEE Commun. Lett.*, vol. 26, no. 2, pp. 249–253, Feb. 2022.

[27] D. Luo, Z. Ye, B. Si, and J. Zhu, "Secure transmit beamforming for radar-communication system without eavesdropper CSI," *IEEE Trans. Veh. Technol.*, vol. 71, no. 9, pp. 9794–9804, Sep. 2022.

[28] N. Su, F. Liu, Z. Wei, Y. Liu, and C. Masouros, "Secure dual-functional radar-communication transmission: Exploiting interference for resilience against target eavesdropping," *IEEE Trans. Wireless Commun.*, vol. 21, no. 9, pp. 7238–7252, Sep. 2022.

[29] Z. Yang, D. Li, N. Zhao, Z. Wu, Y. Li, and D. Niyato, "Secure precoding optimization for NOMA-aided integrated sensing and communication," *IEEE Trans. Commun.*, vol. 70, no. 12, pp. 8370–8382, Dec. 2022.

[30] B. A. Bash, D. Goeckel, and D. Towsley, "Limits of reliable communication with low probability of detection on AWGN channels," *IEEE J. Sel. Areas Commun.*, vol. 31, no. 9, pp. 1921–1930, Sep. 2013.

[31] X. Chen et al., "Covert communications: A comprehensive survey," *IEEE Commun. Surveys Tuts.*, vol. 25, no. 2, pp. 1173–1198, 2nd Quart., 2023, doi: 10.1109/COMST.2023.3263921.

[32] Y. Zhang, Y. Zhang, J. Wang, S. Xiao, and W. Tang, "Distance-angle beamforming for covert communications via frequency diverse array: Towards two-dimensional covertness," *IEEE Trans. Wireless Commun.*, vol. 22, no. 12, pp. 8559–8574, Aug. 2023.

[33] K. Wang, A. M. So, T. Chang, W. Ma, and C. Chi, "Outage constrained robust transmit optimization for multiuser MISO downlinks: Tractable approximations by conic optimization," *IEEE Trans. Signal Process.*, vol. 62, no. 21, pp. 5690–5705, Nov. 2014.

[34] G. Zhou et al., "A framework of robust transmission design for IRS-aided MISO communications with imperfect cascaded channels," *IEEE Trans. Signal Process.*, vol. 68, pp. 5092–5106, 2020.

[35] Y. Huang, H. Fu, S. A. Vorobyov, and Z.-Q. Luo, "Robust adaptive beamforming via worst-case SINR maximization with nonconvex uncertainty sets," *IEEE Trans. Signal Process.*, vol. 71, pp. 218–232, 2023.

[36] Z.-Q. Luo, W.-K. Ma, A. So, Y. Ye, and S. Zhang, "Semidefinite relaxation of quadratic optimization problems," *IEEE Signal Process. Mag.*, vol. 27, no. 3, pp. 20–34, May 2010.

[37] M. Razaviyayn, M. Hong, and Z.-Q. Luo, "A unified convergence analysis of block successive minimization methods for nonsmooth optimization," *SIAM J. Optim.*, vol. 23, no. 2, pp. 1126–1153, Jan. 2013.

Yuchen Zhang (Graduate Student Member, IEEE) received the B.E. degree in communication engineering from the University of Electronic Science and Technology of China (UESTC), Chengdu, China, in 2018, where he is currently pursuing the Ph.D. degree with the National Key Laboratory of Wireless Communications. From 2022 to 2023, he was a Visiting Ph.D. Student with the Department of Computer Science and Applied Mathematics, Weizmann Institute of Science, Rehovot, Israel, under the supervision of Prof. Yonina C. Eldar. His research interests include integrated sensing and communications (ISAC), near-field communications, next-generation multiple access (NGMA), radio localization, and their intersections with convex optimization, security, and privacy.

Wanli Ni (Member, IEEE) received the B.Eng. and Ph.D. degrees from the School of Information and Communication Engineering, Beijing University of Posts and Telecommunications (BUPT), China, in 2018 and 2023, respectively. From September 2020 to June 2022, he was a Visiting Student (remote) with the School of Electronic Engineering and Computer Science, Queen Mary University of London, U.K., under the supervision of Prof. Y. Liu. From July 2022 to September 2022, he was a Visiting Student with the Department of Electrical and Electronic Engineering, Southern University of Science and Technology, Shenzhen, China, under the supervision of Prof. C. You. From December 2022 to June 2023, he was a Visiting Student with the School of Computer Science and Engineering, Nanyang Technological University, Singapore, under the supervision of Prof. D. Niyato. He is currently a Research Assistant with the Department of Electronic Engineering, Tsinghua University, China, under the supervision of Prof. Z. Qin. His research interests include federated learning, reconfigurable intelligent surfaces, nonorthogonal multiple access, over-the-air computation, integrated sensing and communication, machine learning in wireless communications, performance analysis, and optimization of wireless networks. He was a recipient of the Samsung Scholarship in 2019, the National Scholarship in 2021 and 2022, the Excellent Graduate of Beijing in 2023, the BUPT Outstanding Doctoral Dissertation Award in 2023, and the BUPT Top-10 Campus Pioneers on Academic in 2023. He was the coauthor of the Best Paper Award in the IEEE SAGC 2020. He was a recipient of the IEEE ComSoc Student Travel Grant from multiple international conferences, including IEEE GLOBECOM, INFOCOM, and ICC. He was selected as an Exemplary Reviewer of IEEE WIRELESS COMMUNICATIONS LETTERS in 2021, IEEE COMMUNICATIONS LETTERS in 2022, and IEEE TRANSACTIONS ON COMMUNICATIONS in 2022.

Jianquan Wang received the B.S.E. and Ph.D. degrees from the University of Electronic Science and Technology of China, Chengdu, China, in 2013 and 2019, respectively. Currently, he is an Associate Professor with the National Key Laboratory of Wireless Communications, University of Electronic Science and Technology of China. His research interests include covert communication, mobile communication, and low probability of intercept communication.

Wanbin Tang (Member, IEEE) received the B.E., M.E., and Ph.D. degrees in electrical engineering from the University of Electronic Science and Technology of China (UESTC) in 1993, 1998, and 2013, respectively. From 2006 to 2007, he was a Visiting Scholar with the University of California at Berkeley, Berkeley, CA, USA. He is currently a Professor with the National Key Laboratory of Science and Technology on Communications, UESTC. His current research interests include cognitive radio and signal processing in wireless communication.

Min Jia (Senior Member, IEEE) received the M.Sc. degree in information and communication engineering from Harbin Institute of Technology (HIT), Harbin, China, in 2006, and the joint Ph.D. degree from Sungkyungkwan University, Seoul, South Korea, and HIT in 2010. She is currently a Professor and the Ph.D. Supervisor with the School of Electronics and Information Engineering, HIT. Her research interests include advanced mobile communication technology for LTE and 5G, cognitive radios, digital signal processing, and advanced broadband satellite communication systems. She is a member of the Steering Committee of the WiSATs International Conference. She has won six best paper awards at several international conferences. She is the winner of the Science Fund for Excellent Young Scholars for Heilongjiang Province and was elected as a member of the National Major Talent Project. She is the General Chair of the IEEE GLOBECOM 2019 Workshop Intelligent and Cognitive Space, Terrestrial and Ocean Internet, Systems and Applications.

Yonina C. Eldar (Fellow, IEEE) received the B.Sc. degree in physics and the B.Sc. degree in electrical engineering from Tel-Aviv University, Tel-Aviv, Israel, in 1995 and 1996, respectively, and the Ph.D. degree in electrical engineering and computer science from Massachusetts Institute of Technology (MIT), Cambridge, MA, USA, in 2002. She is currently a Professor with the Department of Mathematics and Computer Science, Weizmann Institute of Science, Rehovot, Israel. Her research interests include statistical signal processing, sampling theory and compressed sensing, learning and optimization methods, and their applications to biology, medical imaging, and optics.

Dusit Niyato (Fellow, IEEE) received the B.Eng. degree from the King Mongkuts Institute of Technology Ladkrabang (KMITL), Thailand, in 1999, and the Ph.D. degree in electrical and computer engineering from the University of Manitoba, Canada, in 2008. He is currently a Professor with the School of Computer Science and Engineering, Nanyang Technological University, Singapore. His research interests include sustainability, edge intelligence, decentralized machine learning, and incentive mechanism design.